HEp-2 cells (Table). As anticipated, mutTNF was unable to activate TNFR1. Likewise clones N3 and N7 do not activate TNFR1 signaling, even when tested at high concentrations. The TNFR1-mediated antagonistic assay demonstrated that N7 showed the highest activity of all the TNFR1-selective antagonist candidates. The Figure show details of bioactivities and antagonistic activities of N7. The TNFR1-mediated agonistic activity using L-M cells showed that wtTNF displays TNFR1-mediated agonistic activity in a dose-dependent manner. In contrast, N7, in addition to mutTNF, barely displays any agonistic activity (Fig. A). Moreover, N7 had an almost identical antagonistic activity for TNFR1-mediated bioactivity to that of mutTNF (Fig. B). Next, TNFR2-mediated activities of these TNFR1-selective antagonists were measured using hTNFR2/mFas-preadipocyte cells. The bioactivity of mutTNF and N7 *via* TNFR2 was much lower than that of wtTNF. Remarkably, TNFR2-mediated agonistic activity of N7 was lower than that of mutTNF, in agreement with the reduced affinity for TNFR2 (Fig. C).

In conclusion, we have succeeded in creating a TNFR1-selective antagonist with improved TNFR1-selectivity over that of mutTNF. This was achieved by constructing a library of mutTNF variants using a phage display technique. While TNFR1 is believed to be important for immunological responses (Rothe et al. 1993), TNFR2 is thought to be important for antiviral resistance and is effective for controlling mycobacterial infection by affecting membrane-bound TNF stimulation (Saunders et al. 2005; Olleros et al. 2002). Therefore, use of N7 might reduce the risk of side effects, such as infections, when applying TNF blockade as a therapy for autoimmune disease. We are currently evaluating the therapeutic effect of N7 using a mouse autoimmune disease model.

3. Experimental

3.1. Cell culture

HEp-2 cells (a human fibroblast cell line) were provided by Cell Resource Center for Biomedical Research (Tohoku University, Sendai) and were maintained in RPMI 1640 medium supplemented with 10% FBS and 1% antibiotics cocktail (penicillin 10,000 units/ml, streptomycin 10 mg/ml, and amphotericin B 25 μg/ml). L-M cells (a mouse fibroblast cell line) were provided by Mochida Pharmaceutical Co. Ltd. (Tokyo, Japan) and were maintained in minimum Eagle's medium supplemented with 1% FBS and 1% antibiotics cocktail. hTNFR2/mFas-preadipocyte cells were established previously in our laboratory (Abe et al. 2008) and were maintained in Dulbecco's modified Eagle's medium supplemented with Blasticidin S HCl, 10% FBS, 1 mM sodium pyruvate, 5×10^{-5} M 2-mercaptoethanol, and 1% antibiotic cocktail.

3.2. Construction of a novel gene library displaying mutTNF variants

The pCANTAB phagemid vector encoding mutTNF was used as template for PCR. The mutTNF was created in previous study and showed TNFR1-selective antagonistic activity (Shibata et al. 2008b). The six amino acid residues at the receptor binding site (amino acid residues; 29, 31, 32 and 145–147) of mutTNF were replaced with other amino acids using a 2-step PCR procedure as described previously (Mukai et al. 2009).

3.3. Selection of TNFR1-selective antagonist candidates from a mutTNF mutated phage library

Human TNFR1 Fc chimera (R&D systems, Minneapolis, MN) was immobilized onto a CM3 sensor chip as described previously. Briefly, the phage display library (1×10^{11} CFU/100 μl) was injected over the sensor chip at a flow rate of 3 μl/min. After binding, the sensor chip was washed using the rinse command until the association phase was reached. Elution was carried out using 4 μl of 10 mM glycine-HCl. The eluted phage pool was neutralized with 1 M Tris-HCl (pH 6.9) and then used to infect *E. coli* TG1 in order to amplify the phage. The panning steps were repeated twice. Subsequently, single clones were isolated and supernatant from each clone was collected and used to determine the cytotoxicity in the HEp-2 cytotoxic assay and the affinity for TNFR1 by ELISA, respectively (Shibata et al. 2008b). We screened clones having almost no cytotoxicity but significant affinity for TNFR1. The phagemids purified from single clones were sequenced using the Big Dye Terminator v3.1 kit (Applied Biosystems, Foster City, CA). Sequencing reactions were analyzed on an ABI PRISM 3100 (Applied Biosystems).

3.4. Surface plasmon resonance assay (BIAcore® assay)

The binding kinetics of the proteins were analyzed by the surface plasmon resonance technique by BIAcore® (GE Healthcare, Amersham, UK). Each TNF receptor was immobilized onto a CM5 sensor chip, which resulted in an increase of 3,000–3,500 resonance units. During the association phase, all clones serially diluted in running buffer (HBS-EP) were allowed to pass over TNFR1 and TNFR2 at a flow rate of 20 μl/min. Kinetic parameters for each candidate were calculated from the respective sensorgram using BIAevaluation 4.0 software.

3.5. Cytotoxicity assay

In order to measure TNFR1-mediated cytotoxicity, HEp-2 or L-M cells were cultured in 96-well plates in the presence of TNF mutants and serially diluted wtTNF (Peprotech, Rocky Hill, NJ) with 100 μg/ml cycloheximide for 18 h at $4 \cdot 10^4$ cells/well or for 48 h at $1 \cdot 104$ cells/well. Cytotoxicity was then assessed using the methylene blue assay as described previously (Mukai et al. 2009; Shibata et al. 2004). For the TNFR1-mediated antagonistic assay, cells were cultured in the presence of 5 ng/ml human wtTNF and a serial dilution of the mutTNF. For the TNFR2-mediated cytotoxic assay, hTNFR2/mFas-preadipocyte cells were cultured in 96-well plates in the presence of TNF mutants and serially diluted wtTNF ($1 \cdot 10^4$ cells/well) (Abe et al. 2008). After incubation for 48 h, cell survival was determined using the methylene blue assay.

Acknowledgement: This study was supported in part by Grants-in-Aid for Scientific Research from the Ministry of Education, Culture, Sports, Science and Technology of Japan, and by Grants-in-Aid for Scientific Research from Japan Society for the Promotion of Science (JSPS). In addition, this study was also supported in part by Health Labour Sciences Research Grants from the Ministry of Health, Labor and Welfare of Japan, Health Sciences Research Grants for Research on Publicly Essential Drugs and Medical Devices from the Japan Health Sciences Foundation and by a Grant from the Minister of the Environment, as well as THE NAGAI FOUNDATION TOKYO.

References

Abe Y, Yoshikawa T, Kamada H, Shibata H, Nomura T, Minowa K, Kayamuro H, Katayama K, Miyoshi H, Mukai Y, Yoshioka Y, Nakagawa S, Tsunoda S, Tsutsumi Y (2008) Simple and highly sensitive assay system for TNFR2-mediated soluble- and transmembrane-TNF activity. J Immunol Methods 335: 71–78.

Aggarwal BB (2003) Signalling pathways of the TNF superfamily: a double-edged sword. Nat Rev Immunol 3: 745–756.

Brown SL, Greene MH, Gershon SK, Edwards ET, Braun MM (2002) Tumor necrosis factor antagonist therapy and lymphoma development: twenty-six cases reported to the Food and Drug Administration. Arthritis Rheum 46: 3151–3158.

Feldmann M (2002) Development of anti-TNF therapy for rheumatoid arthritis. Nat Rev Immunol 2: 364–371.

Goldbach-Mansky R, Lipsky PE (2003) New concepts in the treatment of rheumatoid arthritis. Annu Rev Med 54: 197–216.

Gomez-Reino JJ, Carmona L, Valverde VR, Mola EM, Montero MD (2003) Treatment of rheumatoid arthritis with tumor necrosis factor inhibitors may predispose to significant increase in tuberculosis risk: a multicenter active-surveillance report. Arthritis Rheum 48: 2122–2127.

Grell M, Becke FM, Wajant H, Mannel DN, Scheurich P (1998) TNF receptor type 2 mediates thymocyte proliferation independently of TNF receptor type 1. Eur J Immunol 28: 257–263.

Imai S, Mukai Y, Takeda T, Abe Y, Nagano K, Kamada H, Nakagawa S, Tsunoda S, Tsutsumi Y (2008) Effect of protein properties on display efficiency using the M13 phage display system. Pharmazie 63: 760–764.

Kim EY, Priatel JJ, Teh SJ, Teh HS (2006) TNF receptor type 2 (p75) functions as a costimulator for antigen-driven T cell responses *in vivo*. J Immunol 176: 1026–1035.

Kim EY, Teh HS (2001) TNF type 2 receptor (p75) lowers the threshold of T cell activation. J Immunol 167: 6812–6820.

Kollias G, Kontoyiannis D (2002) Role of TNF/TNFR in autoimmunity: specific TNF receptor blockade may be advantageous to anti-TNF treatments. Cytokine Growth Factor Rev 13: 315–321.

Lubel JS, Testro AG, Angus PW (2007) Hepatitis B virus reactivation following immunosuppressive therapy: guidelines for prevention and management. Intern Med J 37: 705–712.

Mori L, Iselin S, De Libero G, Lesslauer W (1996) Attenuation of collagen-induced arthritis in 55-kDa TNF receptor type 1 (TNFR1)-IgG1-treated and TNFR1-deficient mice. J Immunol 157: 3178–3182.

Mukai Y, Shibata H, Nakamura T, Yoshioka Y, Abe Y, Nomura T, Taniai M, Ohta T, Ikemizu S, Nakagawa S, Tsunoda S, Kamada H, Yamagata Y, Tsutsumi Y (2009) Structure-function relationship of tumor necrosis factor (TNF) and its receptor interaction based on 3D structural analysis of a fully active TNFR1-selective TNF mutant. J Mol Biol 385: 1221–1229.

Nagano K, Imai S, Mukai Y, Nakagawa S, Abe Y, Kamada H, Tsunoda S, Tsutsumi Y (2009) Rapid isolation of intrabody candidates by using an optimized non-immune phage antibody library. Pharmazie 64: 238–241.

Nomura T, Kawamura M, Shibata H, Abe Y, Ohkawa A, Mukai Y, Sugita T, Imai S, Nagano K, Okamoto T, Tsutsumi Y, Kamada H, Nakagawa S, Tsunoda S (2007) Creation of a novel cell penetrating peptide, using a random 18mer peptides library. Pharmazie 62: 569–573.

Olleros ML, Guler R, Corazza N, Vesin D, Eugster HP, Marchal G, Chavarot P, Mueller C, Garcia I (2002) Transmembrane TNF induces an efficient cell-mediated immunity and resistance to Mycobacterium bovis bacillus Calmette-Guerin infection in the absence of secreted TNF and lymphotoxin-alpha. J Immunol 168: 3394–3401.

Rothe J, Lesslauer W, Lotscher H, Lang Y, Koebel P, Kontgen F, Althage A, Zinkernagel R, Steinmetz M, Bluethmann H (1993) Mice lacking the tumour necrosis factor receptor 1 are resistant to TNF-mediated toxicity but highly susceptible to infection by Listeria monocytogenes. Nature 364: 798–802.

Saunders BM, Tran S, Ruuls S, Sedgwick JD, Briscoe H, Britton WJ (2005) Transmembrane TNF is sufficient to initiate cell migration and granuloma formation and provide acute, but not long-term, control of Mycobacterium tuberculosis infection. J Immunol 174: 4852–4859.

Shibata H, Yoshioka Y, Ikemizu S, Kobayashi K, Yamamoto Y, Mukai Y, Okamoto T, Taniai M, Kawamura M, Abe Y, Nakagawa S, Hayakawa T, Nagata S, Yamagata Y, Mayumi T, Kamada H, Tsutsumi Y (2004) Functionalization of tumor necrosis factor-alpha using phage display technique and PEGylation improves its antitumor therapeutic window. Clin Cancer Res 10: 8293–8300.

Shibata H, Yoshioka Y, Ohkawa A, Abe Y, Nomura T, Mukai Y, Nakagawa S, Taniai M, Ohta T, Mayumi T, Kamada H, Tsunoda S, Tsutsumi Y (2008a) The therapeutic effect of TNFR1-selective antagonistic mutant TNF-alpha in murine hepatitis models. Cytokine 44: 229–233.

Shibata H, Yoshioka Y, Ohkawa A, Minowa K, Mukai Y, Abe Y, Taniai M, Nomura T, Kayamuro H, Nabeshi H, Sugita T, Imai S, Nagano K, Yoshikawa T, Fujita T, Nakagawa S, Yamamoto A, Ohta T, Hayakawa T, Mayumi T, Vandenabeele P, Aggarwal BB, Nakamura T, Yamagata Y, Tsunoda S, Kamada H, Tsutsumi Y (2008b) Creation and X-ray structure analysis of the tumor necrosis factor receptor-1-selective mutant of a tumor necrosis factor-alpha antagonist. J Biol Chem 283: 998–1007.

Yamamoto Y, Tsutsumi Y, Yoshioka Y, Nishibata T, Kobayashi K, Okamoto T, Mukai Y, Shimizu T, Nakagawa S, Nagata S, Mayumi T (2003) Site-specific PEGylation of a lysine-deficient TNF-alpha with full bioactivity. Nat Biotechnol 21: 546–552.

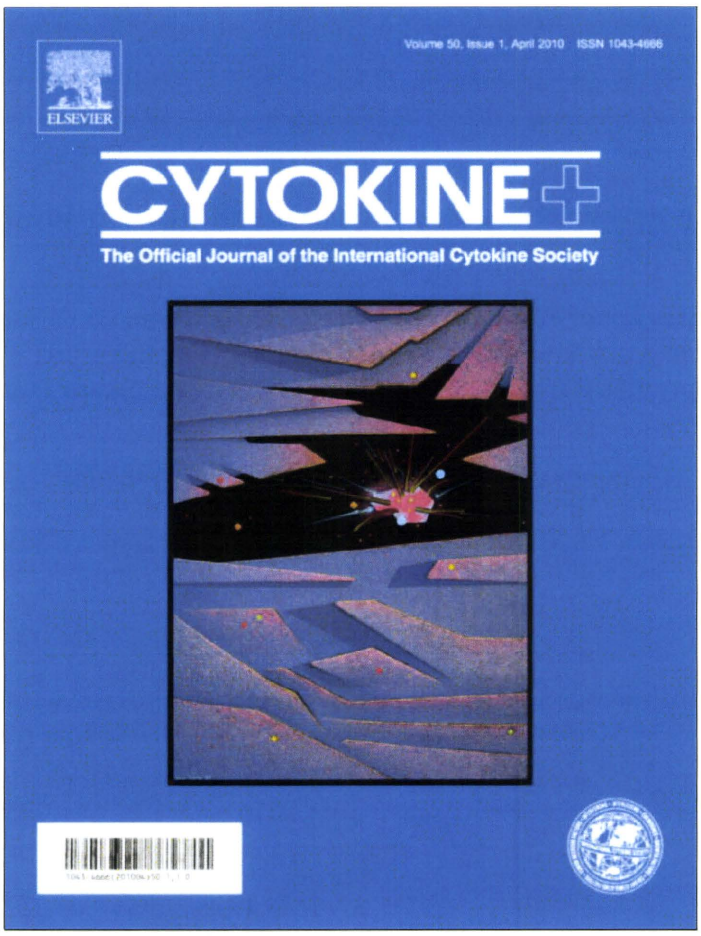

Cytokine 50 (2010) 75–83

Contents lists available at ScienceDirect

Cytokine

journal homepage: www.elsevier.com/locate/issn/10434666

Generation of mouse macrophages expressing membrane-bound TNF variants with selectivity for TNFR1 or TNFR2

Hiroko Shibata [a,b,1], Yasuhiro Abe [a,1], Yasuo Yoshioka [a,c,1], Tetsuya Nomura [a,d], Masaki Sato [a], Hiroyuki Kayamuro [a,d], Tomoyuki Kawara [a,d], Shuhei Arita [a,d], Tsuyoshi Furuya [a,d], Kazuya Nagano [a], Tomoaki Yoshikawa [a,d], Haruhiko Kamada [a,c], Shin-ichi Tsunoda [a,c,d,*], Yasuo Tsutsumi [a,c,d]

[a] National Institute of Biomedical Innovation (NiBio), 7-6-8 Saito-Asagi, Ibaraki, Osaka 567-0085, Japan
[b] National Institute of Health Science (NIHS), Kamiyoga 1-18-1, Setagaya-ku, Tokyo 158-8501, Japan
[c] The Center for Advanced Medical Engineering and Informatics, Osaka University, 1-6 Yamadaoka, Suita, Osaka 565-0871, Japan
[d] Graduate School of Pharmaceutical Sciences, Osaka University, 1-6 Yamadaoka, Suita, Osaka 565-0871, Japan

ARTICLE INFO

Article history:
Received 31 July 2009
Received in revised form 6 November 2009
Accepted 24 November 2009

Keywords:
Transmembrane TNF
TNFR1
TNFR2
Mutant TNF
Lentiviral vector

ABSTRACT

Tumor necrosis factor-alpha (TNF) is expressed on the cell surface as a transmembrane form (tmTNF), that can be released as a soluble form (solTNF) via proteolytic cleavage. These two types of TNF exert their biological functions by binding to one of two TNF receptors, TNFR1 or TNFR2. However, the biological function of tmTNF through these two receptors remains to be determined. Here, we generated macrophages that expressed tmTNF mutants with selectivity for either TNFR1 or TNRF2 as a tool to evaluate signaling through these receptors. Wild-type TNF (wtTNF), TNFR1-selective mutant TNF (mutTNF-R1) or TNFR2-selective mutant TNF (mutTNF-R2) were individually expressed on the TNFR1$^{-/-}$R2$^{-/-}$ mouse macrophages (Mφ) as the tmTNF forms. tm-mutTNF-R1-expressing Mφ exhibited significant selectivity for binding to TNFR1, whereas tm-mutTNF-R2-expressing Mφ only showed a slight selectivity for binding to TNFR2. Signaling by tm-mutTNF-R1-expressing Mφ through the hTNFR2 was weaker than that of tm-wtTNF-expressing Mφ, suggesting that the binding selectivity correlated with functional selectivity. Interestingly, signaling by tm-mutTNF-R2-expressing Mφ through TNFR2 was much stronger than signaling by tm-wtTNF-expressing Mφ, whereas signaling by the corresponding soluble form was weaker than that mediated by wtTNF. These results indicate tmTNF variants might prove useful for the functional analysis of signaling through TNF receptors.

1. Introduction

Tumor necrosis factor alpha (TNF) plays a crucial role in the host defense system [1]. Increased secretion of TNF is involved in the development of autoimmune diseases, such as rheumatoid arthritis (RA) and Crohn's disease [2,3]. Indeed, anti-human TNF antibody and soluble TNF receptor (TNFR), which interfere with the activity of TNF, have been used to treat these diseases, and are expected to be revolutionary therapies due to their excellent therapeutic effects [4]. TNF is primarily produced as a type II transmembrane form (tmTNF) arranged in stable homotrimers [5,6]. A mature, soluble homotrimeric 17-kDa TNF (solTNF) is released from this 26 kDa memTNF *via* proteolytic cleavage by the metalloprotease, TNF converting enzyme (TACE) [7]. Both solTNF and tmTNF induce cell signaling. tmTNF acts through cell–cell contacts to promote juxtacrine signaling, and solTNF acts in a paracrine fashion. The relative contribution of tmTNF and solTNF to overall TNF activity is difficult to elucidate due to the absence of physiologically relevant models. However, evidence for distinct roles for tmTNF and solTNF *in vivo* have been obtained in genetically modified mice. Study of tmTNF knock-in mice revealed that solTNF is required for the development of acute and chronic inflammation, whereas tmTNF supports many processes underlying the development of lymphoid tissue [8]. Mueller et al. also reported that tmTNF has a strong effect upon the course of cellular immune responses *in vivo* and exerts quantitatively and qualitatively distinct functions from solTNF *in vitro* and *in vivo* [9]. Additionally, juxtacrine signaling by tmTNF was shown to be essential for the resolution of inflammation and the maintenance of immunity to the pathogens, *Listeria monocytogenes* and *Mycobacterium tuberculosis* [10–12]. These different functions mediated by the two forms of TNF may help to explain the opposing activities of TNF, such as

* Corresponding author. Address: National Institute of Biomedical Innovation, Laboratory of Pharmaceutical Proteomics, 7-6-8 Saito-Asagi, Ibaraki, Osaka 567-0085, Japan. Tel.: +81 72 639 7014; fax: +81 72 641 9817.
E-mail address: tsunoda@nibio.go.jp (S.-i. Tsunoda).
[1] These authors contributed equally to this work.

1043-4666/$ - see front matter © 2009 Elsevier Ltd. All rights reserved.
doi:10.1016/j.cyto.2009.11.022

its inflammatory and anti-inflammatory effects. However, the factors underlying the different functions of solTNF and tmTNF and the components of the specific signaling cascades induced by the two forms of TNF remain to be elucidated.

solTNF and tmTNF interact with two receptor subtypes, p55 TNF receptor (TNFR1) and p75 TNF receptor (TNFR2) [13], to exert their biological functions. The interaction of solTNF with TNFR and the downstream signaling and functional outcome of that signaling has been extensively studied [14], because signaling by solTNF *via* TNFR1 or TNFR2 can be analyzed *in vitro* using recombinant wild-type TNF, as well as recombinant TNFR1-, and TNFR2-selective mutant TNF (mutTNF). On the other hand, the analysis of tmTNF/TNFR signaling is still poorly understood. tmTNF-expressing cells have previously been reported following transfection into target cells of a TNF gene containing a deletion of the TNF cleavage site [15]. Nanoparticles decorated with solTNF chemically bound to the surface initiate strong TNFR2 responses, and could mimic the bioactivity of tmTNF [16]. However, there are no receptor-selective forms of tmTNF that could be used to analyze tmTNF/TNFR signaling. Moreover, there are few assay systems that can assess the bioactivity of TNF mediated *via* TNFR2 with high sensitively.

In this context, we have used a novel phage-display based screening system to develop TNFR1 or TNFR2-selective mutTNFs to help clarify the biology of TNF/TNFRs interactions. We have already isolated a TNFR1-selective antagonist [17], and both TNFR1 and TNFR2-selective agonists [18]. Additionally, we established a novel cell line hTNFR2/mFas-preadipocyte, which is a simple and highly sensitive, cell death-based assay system for measuring TNFR2-mediated bioactivity [19]. This assay system can assess both solTNF and tmTNF-mediated bioactivity. In this study, we first expressed the TNFR-selective mutTNFs agonists (mutTNF-R1, mutTNF-R2) in TNFR1$^{-/-}$R2$^{-/-}$ macrophages, and we then investigated the possibility of creating TNFR1- and TNFR2-selective tmTNF.

2. Materials and methods

2.1. Cells

The immortalized TNFR1$^{-/-}$R2$^{-/-}$macrophage cell line (DKO Mφ) established from the bone marrow of a TNFR1$^{-/-}$R2$^{-/-}$ mouse was generously provided by Dr. Aggarwal (The University of Texas M.D. Anderson Cancer Center, Houston TX), and cultured in RPMI-1640 medium supplemented with 10% fetal bovine serum (FBS) and 1% antibiotic cocktail (penicillin 10,000 U/ml, streptomycin 10 mg/ml, and amphotericin B 25 μg/ml; Nacalai Tesque, Kyoto, Japan). Human-TNFR2/mouse-Fas-expressing preadipocytes (hTNFR2/mFas-PA) were maintained in Dulbecco's modified Eagle's medium (DMEM; Sigma–Aldrich, Inc., Tokyo, Japan) with 10% FBS, 1% antibiotic cocktail, and 5 μg/ml blasticidin (Bsd) (Invitrogen Corp., Carlsbad, CA). hTNFR2/mFas-PA cells express a chimeric receptor derived from the extracellular and transmembrane domain of human TNFR2 fused to the intracellular domain of mouse Fas [19]. 293T cells and HeLaP4 cells were cultured in DMEM with 10% FBS and 1% antibiotic cocktail. HEp-2 cells are a human laryngeal squamous cell carcinoma cell line, and were cultured in RPMI-1640 medium supplemented with 10% FBS and 1% antibiotic cocktail.

2.2. Surface plasmon resonance (SPR) assay

The binding kinetics of wtTNF, mutTNF-R1 and mutTNF-R2 were analyzed by the SPR technique using a BIAcore 3000 (BIAcore®, GE Healthcare, Buckinghamshire, UK). Human TNFR1 or human TNFR2 Fc chimeras (R&D systems, Minneapolis, MN) were diluted to 50 μg/ml in 10 mM sodium acetate buffer (pH 4.5). TNFRs were immobilized on a CM5 sensor chip, which resulted in an increase of 3000–3500 resonance units (RU). During the association phase, TNFs diluted in running buffer (HBS-EP) at 156.8, 52.3 or 17.4 nM were individually passed over the immobilized TNFRs at a flow rate of 20 μl/min. During the dissociation phase, HBS-EP buffer was applied to the sensor chip at a flow rate of 20 μl/min. The data were analyzed with BIAEVALUATION 3.0 software (BIAcore®) using a 1:1 binding model.

2.3. Cytotoxicity assays

HEp-2 cells were cultured in 96-well plates (4×10^4 cells/well) in a serial dilution of human TNF (Peprotech, Rocky Hill, NJ) or mutTNFs with 100 μg/ml cycloheximide. After incubation for 18 h, cell survival was determined using the methylene blue assay as described previously [17]. hTNFR2/mFas-PA were seeded onto 96-well plates at a density of 1.5×10^4 cells/well in culture medium. Serial dilutions of human TNF or paraformaldehyde-fixed Mφ cells were prepared in DMEM containing 1 μg/ml cycloheximide, and added to each well. After 48 h, cell viability was measured using the WST-assay kit (Nacalai Tesque) according to the manufacturer's instructions.

2.4. Construction of a self-inactivating (SIN) lentiviral vector

Vectors were constructed using standard cloning procedures. A DNA fragment encoding the precursor signal of human TNF was amplified by polymerase chain reaction (PCR) with the following primer pairs : forward primer-1 (5′-GAT TTC GAT ACG TAC GGA AGC TTC GTC GAC ATT AAT TAA GGA CAC CAT GAG CAC TGA AAG CAT GAT CCG GGA CGT GGA GCT GGC CGA GGA GG-3′) containing a SalI site at the 5′-end, reverse primer-1 (5′-AGA GGC TGA GGA ACA AGC ACC GCC TGG AGC CCT GGG GCC CCC CTG TCT TCT TGG GGA GCG CCT CCT CGG CCA GCT CCA CGT CCC GGA TCA-3′), forward primer-2 (5′-GCT CCA GGC GGT GCT TGT TCC TCA GCC TCT TCT CCT TCC TGA TCG TGG CAG GCG CCA CCA CGC TCT TCT GCC TGC TGC ACT TTG GAG TGA-3′), and reverse primer-2 (5′-TGC CTG GGC CAG AGG GCG CGG CCG CGA GAT CTC TGG GGA ACT CTT CCC TCT GGG GGC CGA TCA CTC CAA AGT GCA GCA GGC AGA AGA GCG-3′) containing BglII site at the 5′-end. The resulting amplified fragment was subcloned into the pY02 vector to generate pY02-preTNF. DNA fragments encoding non-cleavable wild-type human TNF (tm-wtTNFΔ1–12) (Fig. 2a), TNFR1-selective mutant TNF (tm-mutTNF-R1Δ1–12), and TNFR2-selective mutant TNF (tm-mutTNF-R2Δ1–12) which were generated by deleting amino acids 1–12 in the N-terminal part of TNF, were amplified by PCR from wtTNF, mutTNF-R1, and mutTNF-R2 respectively with the following primer pairs : forward primer-3 (5′-AGT GAT CGG CCC CCA GAG GGA AGC TTA GAT CTC TCT CTA ATC AGC CCT CTG GCC CAG GCA GTA GCC CAT GTT GTA GCA AAC CCT CAAG-3′) containing a BglII site at the 5′-end, and reverse primer-3 (5′-GGT TGG ATG TTC GTC CTC CGC GGC CGC CTA ACT AGT TCA CAG GGC AAT GAT CCC AAA GTA GAC CTG-3′) containing a NotI site at the 5′-end. These fragments were cloned into the pY02-preTNF vector. Then, fragments of tm-wtTNFΔ1–12, tm-mutTNF-R1Δ1–12, and tm-mutTNF-R2Δ1–12 were cloned between the SalI and NotI sites of the SIN vector construct, generating CSII-EF-tm-wtTNF-IRES-GFP, CSII-EF-tm-mutTNF-R1-IRES-GFP, and CSII-EF-tm-mutTNF-R2-IRES-GFP, respectively.

2.5. Preparation of lentiviral vectors

Lentiviral vectors were prepared as previously described [20,21]. In brief, 293T cells were transfected by the calcium phosphate method with three plasmids: packaging construct (pCAG-HIVgp), VSV-G and Rev expressing construct (pCMV-VSV-G-RSV-Rev) and

the SIN vector constructs (CSII-EF-tm-wtTNF-IRES-rhGFP, CSII-EF-tm-mutTNF-R1-IRES-rhGFP or CSII-EF-tm-mutTNF-R2-IRES-rhGFP) (Fig. 2b). Two days after transfection, the conditioned medium was collected and the virus was concentrated by ultracentrifugation at 50,000*g* for 2 h at 20 °C. The pelleted virus was re-suspended in Hank's balanced salt solution (GIBCO BRL, Paisley, UK). Vector titers were determined by measuring the infectivity of HeLaP4 cells with serial dilutions of vector stocks using flow cytometric analysis (FCM) for GFP-positive cells.

2.6. Creation of membrane-bound TNF expressing cells

To prepare tmTNF-expressing cells, DKO Mφ (1×10^3 cells/well) cells were transfected with each lentiviral vector (tm-wtTNF, tm-mutTNF-R1 or tm-mutTNF-R2) at a multiplicity of infection (MOI) of 160 in 96-well plates. Infected cells were cultured until reaching 1×10^7 cells. IRES-driven GFP-positive cells were single-cell-sorted by FACSVantage™ (BD Biosciences, Franklin Lakes, NJ), and cultured in conditioned medium from DKO Mφ cells. After blocking Fc receptors with anti-mouse CD16/32 (eBioscience, San Diego, CA), the expression of tmTNF on monoclonal cell lines was detected by staining with Phycoerythrin-conjugated anti-human TNF antibody (clone MAb11, eBioscience) at 0.5 μg/5×10^5 cells for 30 min on ice. Subsequently, the cells were washed with 1% FBS/PBS and re-suspended in 500 μl of 4% paraformaldehyde. GFP or phycoerythrin fluorescence was analyzed using FCM by FACSCalibur™. Monoclonal cell lines stably expressing tmTNF or its mutants and GFP (tmTNF-expressing Mφ, tm-wtTNF Mφ, tm-mutTNF-R1 Mφ, or tm-mutTNF-R2 Mφ) were used for the following experiments.

2.7. Measurement of receptor binding activity by FCM

To detect the binding of soluble human TNFR1 (shTNFR1) or TNFR2 (shTNFR2) to tmTNF on Mφ cell lines, shTNFR1- or shTNFR2-Fc chimera were labeled with R-phycoerythrin by Zenon™ Human IgG Labeling Kits (Invitrogen Corp.) according to the manufacturer's procedure. Briefly, 10 μl of shTNFR1- or shTNFR2-Fc chimera (250 μg/ml) (R&D systems) was incubated with 5 μl labeling reagent for 5 min at room temperature, and 5 μl blocking reagent was added to each reaction solution. After incubation for 5 min at room temperature, 4 μl each reaction solution was added to 5×10^5 cells/tube which were pretreated with mouse Fc block. After incubation for 30 min on ice, the cells were washed with 1% FBS/PBS, and then suspended in 500 μl of 0.4% paraformaldehyde.

3. Results and discussion

An understanding of the bioactivity of tmTNF is key to a better understanding of the overall function of TNF and TNF receptors. The relative contribution of signaling by tmTNF through the TNFR1 and TNFR2 receptors is unclear, as it is difficult to monitor the specific activation of these two receptors in response to tmTNF. To address this problem, we established macrophage cell lines expressing TNFR-selective mutant TNFs (tmTNF-R1 or tmTNF-R2) on the cell surface.

First, to assess the receptor selectivity of soluble mutTNF-R1 or R2 (sol-mutTNF-R1 or R2), which we previously created using a phage display system [18], we measured human TNFR1-mediated bioactivities of sol-mutTNFs on HEp-2 cells and human TNFR2-mediated bioactivities on hTNFR2/mFas-PA cells (Fig. 1a and Table 1). The binding affinity and kinetic parameters of these mutant TNFs for each TNF receptor were also measured using a Surface plasmon resonance assay (Fig. 1b and Table 1). We observed that both the bioactivity and binding affinity of sol-mutTNF-R1 for hTNFR1 were equivalent to those of sol-wtTNF, whereas the activity and affinity of sol-mut-TNF-R1 for hTNFR2 were decreased to less than 0.2% and 8%, respectively, of the values observed with sol-wtTNF. Although the bioactivity of sol-mutTNF-R2 mediated via hTNFR2 was only 16% of that of sol-wtTNF, the binding affinity of sol-mutTNF-R2 for human TNFR2 was about 1.5 times higher than that of sol-wtTNF. The bioactivity and binding affinity of sol-mutTNF-R2 for hTNFR1 were decreased to less than 0.1% and 3%, respectively, of the corresponding values for sol-wtTNF. Interestingly, the kinetic parameters, k_{on} and k_{off}, of the sol-mutTNFs for the TNF receptors tended to be higher than those of sol-wtTNF, indicating rapid association/dissociation interaction. From these data, we confirmed a significant TNFR-selectivity of sol-mutTNF-R1 and sol-mutTNF-R2. Therefore, we attempted to create the corresponding TNFR-selective tmTNFs using these sol-mutTNFs.

To express only tmTNF on the cell surface, the recombinant genes corresponding to each sol-TNF mutant, each encoding a protein with an additional twelve amino acid deletion from the N-terminus, were subcloned into lentiviral vectors (Fig. 2a and b). The resulting recombinant lentiviral vectors were transduced into $TNFR1^{-/-}R2^{-/-}$ macrophages (DKO Mφ). As previously reported, the deletion of the first 12 amino acids from the N-terminus of TNF, including the entire TACE cleavage site, leads to the expression of only the tmTNF form, and not the soluble form [15,22]. Since the SIN vector also comprises a GFP expression cassette, GFP expression was visible in all three cell lines: wtTNF-expressing DKO Mφ (tm-wtTNF Mφ), mutTNF-R1 expressing DKO Mφ (tm-mutTNF-R1 Mφ), and mutTNF-R2 expressing DKO Mφ (tm-mutTNF-R2 Mφ) (Fig. 2c). We next verified the expression of TNF on single sorted cells using FCM analysis. We observed significant expression of TNF on tm-wtTNF Mφ (Fig. 3a). The mean fluorescence intensity (MFI) of tm-mutTNF-R1 Mφ and tm-mutTNF-R2 Mφ was lower than that of tm-wtTNF Mφ (Fig. 3b). Since the expression level of GFP on tm-mutTNF-R1 Mφ and tm-mutTNF-R2 Mφ was lower than that on tm-wtTNF Mφ (Fig. 2c), the expression level of TNF on these cells might also be lower than that on tm-wtTNF Mφ.

Next, the affinity of each cell-surface expressed tmTNF for soluble TNF receptors was measured by FCM analysis (Fig. 4a), and receptor selectivity was estimated (Fig. 4b and c). We observed that both soluble TNFR1 and TNFR2 Fc chimeras bound to tm-wtTNF Mφ, although TNFR2 bound to tm-wtTNF Mφ with an affinity approximately twofold stronger than that of TNFR1 (Fig. 4b). Although the affinity of tm-mutTNF-R1 Mφ for TNFR1 was 50% that of tm-wtTNF Mφ, the affinity of tm-mutTNF-R1 Mφ for TNFR2 was greatly decreased and the ratio of selectivity of tm-mutTNF-R1 Mφ for TNFR1 over TNFR2 (R1/R2 of MFI) was approximately three times that of tm-wtTNF Mφ (Fig. 4b and c). Therefore, the expression of mutTNF-R1 on the cell surface as the tmTNF form demonstrates TNFR1 selectivity, as does its soluble form. On the other hand, the affinity of TNFR1 and TNFR2 for tm-mutTNF-R2 Mφ was weaker than their affinity for tm-wtTNF Mφ (Fig. 4a and b). Additionally, the ratio of selectivity of tm-mutTNF-R2 Mφ for TNFR1 over TNFR2 was similar to that of tm-wtTNF Mφ, indicating little selectivity for TNFR2 in contrast to what was observed for sol-mutTNF-R2 (Fig. 4c). We next evaluated the bioactivity of these tmTNFs via hTNFR2, by assessing the cytotoxicity of these tmTNFs on hTNFR2/mFas-PA cells, which express the hTNFR2/mFas chimeric receptor (Fig. 5). As previously reported, a cytotoxicity assay using hTNFR2/mFas-PA cells is a simple and highly sensitive assay system for determining TNFR2-mediated activity. DKO Mφ expressing each type of tmTNF (effector cell) were fixed with paraformaldehyde, and co-cultured with hTNFR2/mFas-PA cells (target cell). The viability of the target cells decreased significantly and in a dose-dependent manner

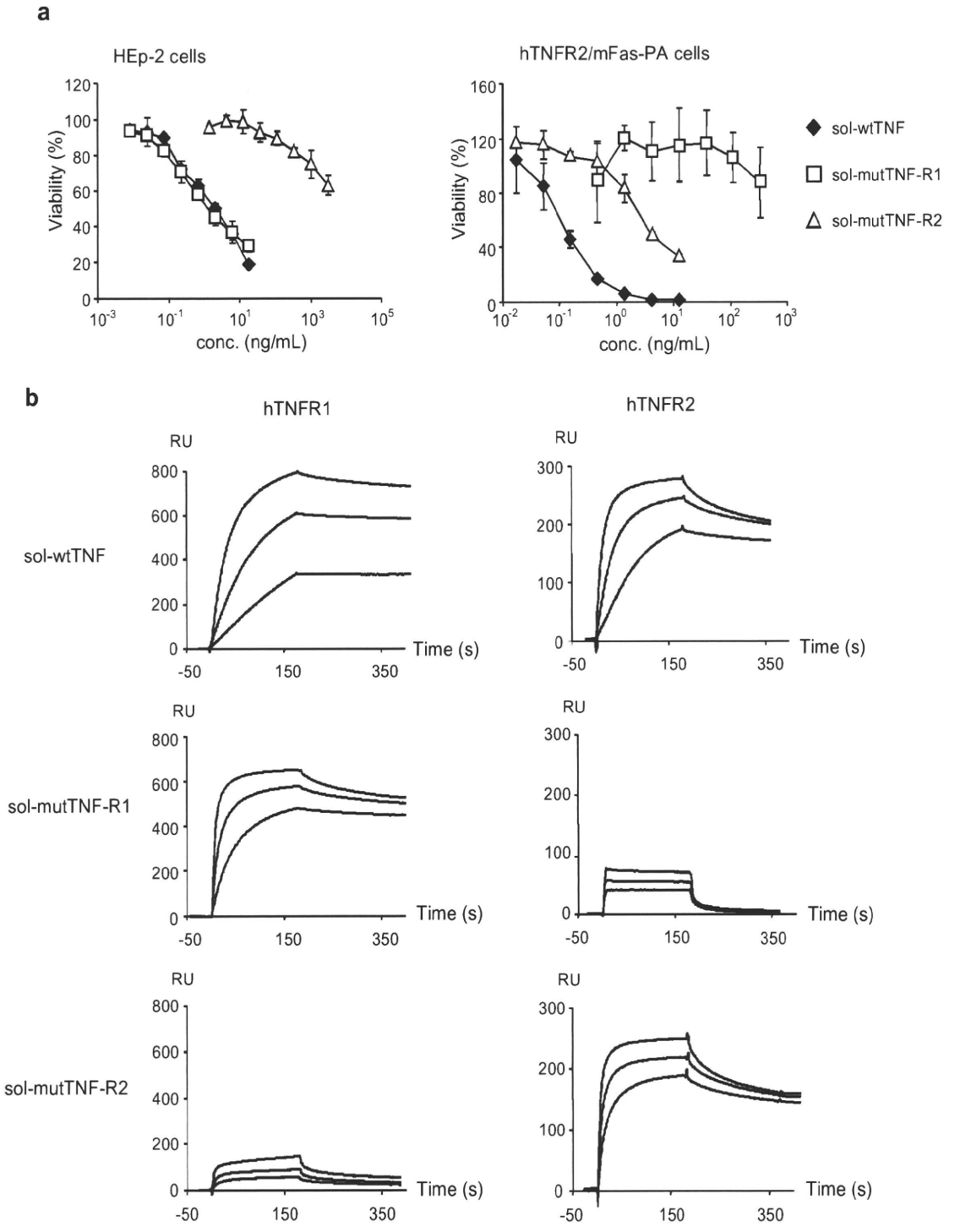

Fig. 1. Bioactivity and binding of sol-wtTNF, sol-mutTNF-R1, and sol-muTNF-R2 to TNFRs. (a) HEp-2 cells or hTNFR2/Fas-PA cells were used for measuring TNFR1-mediated or TNFR2-mediated bioactivity respectively. HEp-2 cells were cultured in serial dilutions of sol-wtTNF, sol-mutTNF-R1, and sol-mutTNF-R2 with 100 μg/ml cycloheximide for 18 h. hTNFR2/Fas-PA cells were also cultured in serial dilutions of sol-TNFs with 1 μg/ml cycloheximide for 48 h. Cell viability was determined using the methylene blue assay for HEp-2 cells, and the WST-8 assay for hTNFR2/Fas-PA cells. (b) The binding kinetics of sol-TNFs to immobilized TNFRs were analyzed using the surface plasmon resonance (SPR) technique. TNFRs were immobilized to a sensor chip CM5, which resulted in an increase of 3000–3500 resonance units (RU). The amount of protein bound to the surface was recorded in RU. Duplicate injections of 156.8, 52.3, or 17.4 nM sol-TNFs were passed over the immobilized TNFRs at a flow rate of 20 μl/min. The sensorgrams shown were normalized by subtracting the control surface sensorgram.

when exposed to an increasing *E*(effector)/*T*(target) cell ratio of tm-wtTNF Mφ compared to exposure to the control DKO Mφ. These results suggest that tmTNF induced death of these cells in a dose-dependent manner via signaling through the TNFR2/mFas chimera expressed on the target cell surface. The bioactivity of tm-mutTNF-R1 Mφ was lower than that of tm-wtTNF Mφ in

Table 1
Amino acid sequence, bioactivity, and kinetic parameters of mutTNFs.

Human TNFs	Amino acids sequence						Bioactivity EC50 (nM)		Binding property					
									TNFR1			TNFR2		
	29	31	32	145	146	147	HEp-2	hTNFR2/ mFas-PA	k_{on} (M^{-1} S^{-1})[a]	k_{off} (s^{-1})[b]	k_d (nM)[c]	k_{on} (M^{-1} S^{-1})[a]	k_{off} (S^{-1})[b]	k_d (nM)[c]
sol-wtTNF	L	R	R	A	E	S	1.9 (100%)	0.5 (100%)	2.1×10^5	1.4×10^{-4}	0.68 (100%)	1.1×10^6	7.8×10^{-4}	0.70 (100%)
sol-mutTNF-R1	K	A	G	A	S	T	1.5 (128%)	>300 (<0.2%)	6.5×10^5	4.7×10^{-4}	0.73 (93%)	5.8×10^6	522.0×10^{-4}	9.0 (8%)
sol-mutTNF-R2	L	R	R	R	E	T	>3000 (<0.1%)	3.1 (16%)	1.8×10^5	36.1×10^{-4}	20.2 (3%)	3.1×10^6	15.4×10^{-4}	0.49 (144%)

Kinetic parameters for each TNF were calculated by from the respective sensorgrams by BIA evaluation 3.0 software. Value in parenthesis shows the relative bioactivity or relative binding affinity (%).
[a] k_{on} is association kinetic constant.
[b] k_{off} is dissociation kinetic constant.
[c] k_d (equilibrium dissociation constant) denotes binding affinity.

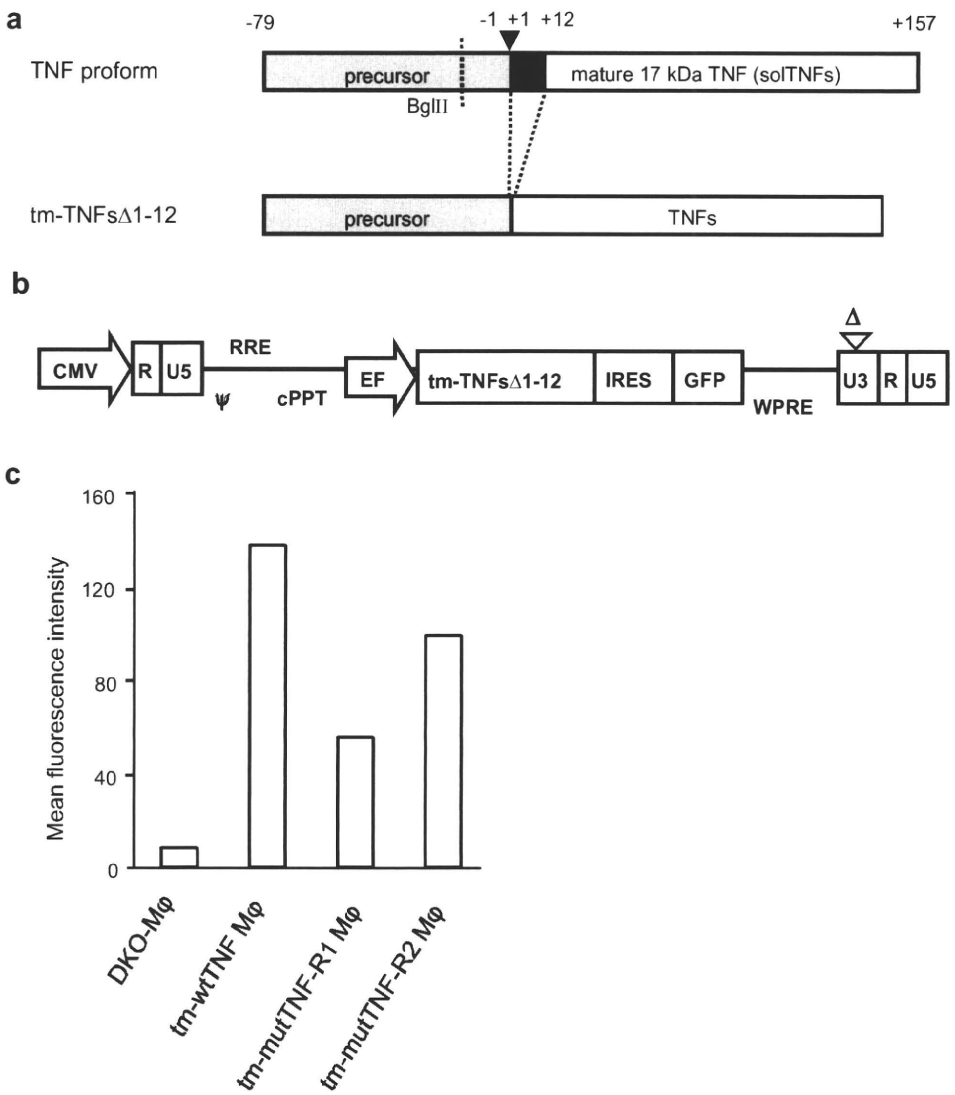

Fig. 2. Schematic representation of the tmTNF forms and the construction of the lentiviral vector. (a) Schematic representation of non-cleavable human TNFs (tm-TNFsΔ1–12). An inverted filled triangle shows the cleavage site. Closed bar, amino acids 1–12, indicates the deleted region. (b) Schematic representation of self-inactivating (SIN) LV plasmid (CSII-EF-tm-TNFsΔ1–12-IRES-GFP). CMV: cytomegalovirus promoter, ψ: packaging signal, RRE: rev responsive element, cPPT: central polypurine tract, IRES: Encephalomyocarditis virus internal ribosomal entry site, Bsd: Blasticidin, WPRE: woodchuck hepatitis virus posttranscriptional regulatory element. Δ: deletion of 133 bp in the U3 region of the 3′ long terminal repeat. (c) Expression of GFP on each cell was analyzed by FCM, and the mean fluorescence intensity of each cell is shown.

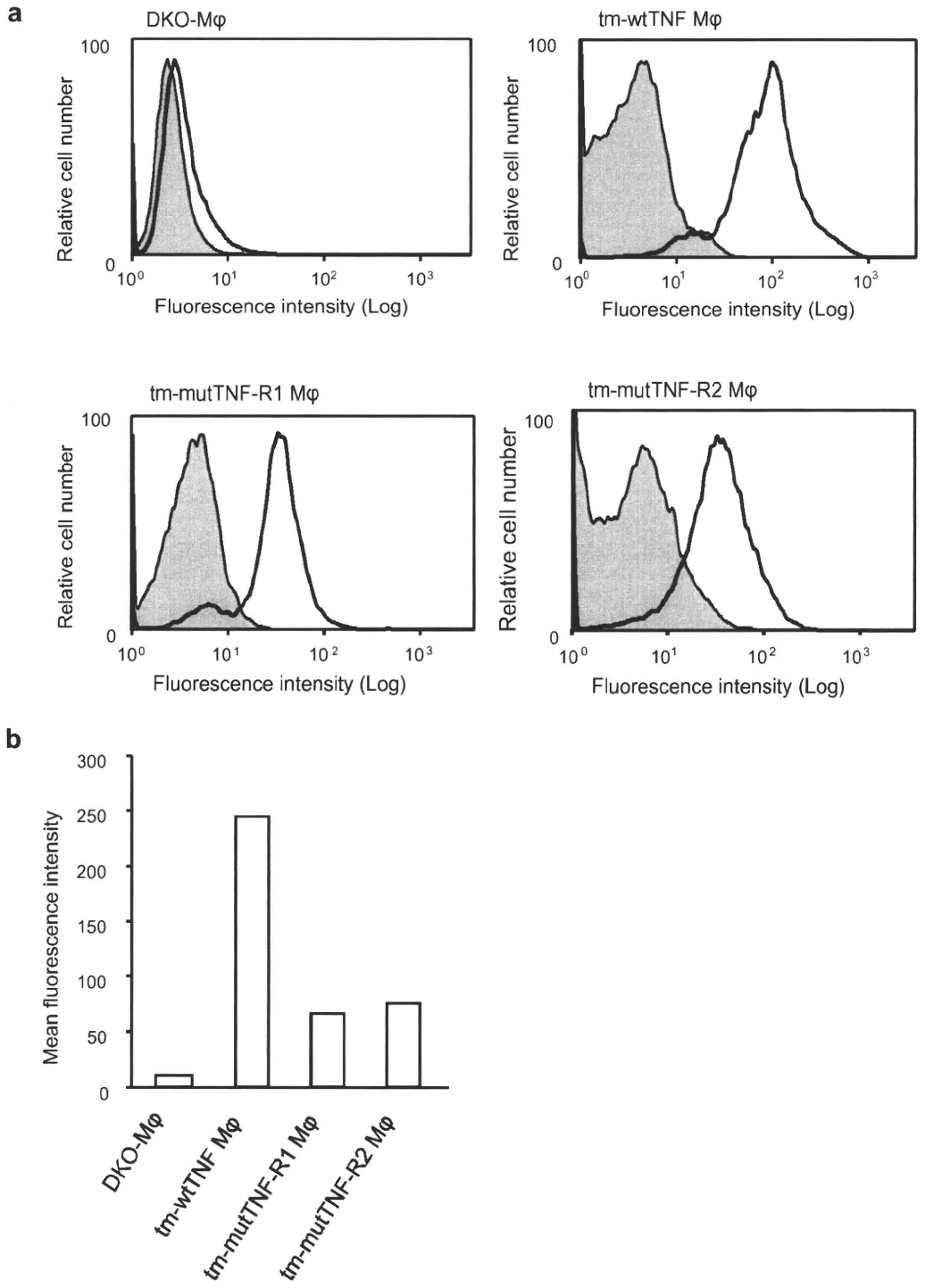

Fig. 3. The expression of TNF as the transmembrane form on tm-TNFs Mφ. (a) Expression of TNF on each cell was analyzed by FCM using PE-conjugated anti-hTNF monoclonal antibody (open histograms) or PE-conjugated isotype control antibody (shaded histograms). (b) The mean fluorescence intensity of each cell is shown.

this assay, which correlates with the results observed when studying its soluble form in Table 1. Interestingly, tm-mutTNF-R2 Mφ was more cytotoxic than tm-wtTNF Mφ, whereas the cytotoxicity of sol-mutTNF-R2 was only 16% of that of sol-wtTNF in this assay.

In this study, we have established the selectivity of tm-mutTNF-R1 Mφ for binding to TNFR1, although we need to measure the precise expression level of TNF in each cell. In addition, FCM analysis suggested that tm-mutTNF-R2 Mφ have a lower affinity for both TNFRs than do tm-wtTNF Mφ, and that they exhibit little selectivity

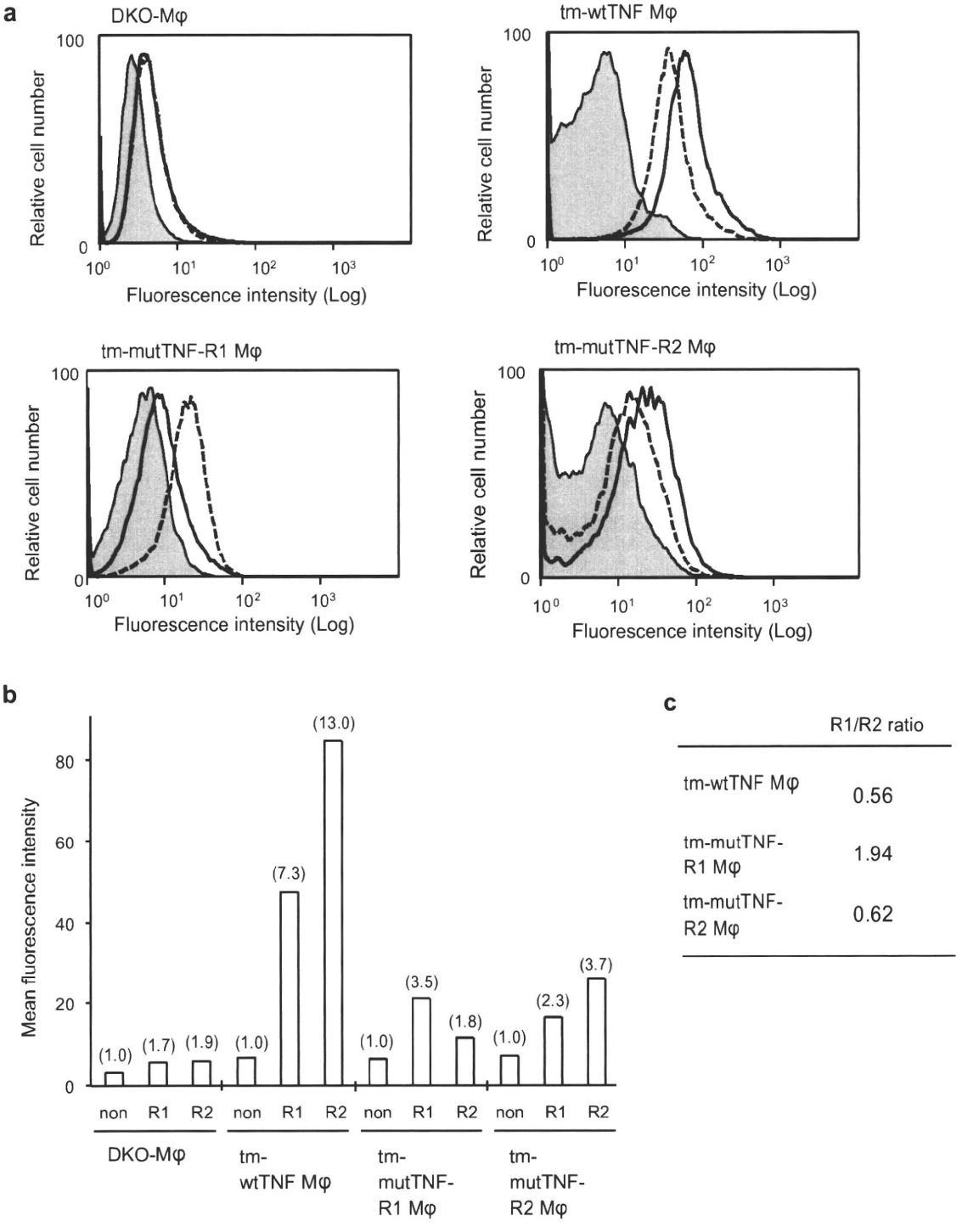

c

	R1/R2 ratio
tm-wtTNF Mφ	0.56
tm-mutTNF-R1 Mφ	1.94
tm-mutTNF-R2 Mφ	0.62

Fig. 4. The affinity of tm-TNFs Mφ for soluble TNF-receptors. (a) The binding of each tmTNF to solTNFR1 (dashed lines) or solTNFR2 (solid lines) was analyzed by FCM analysis. DKO Mφ, tm-wtTNF Mφ, tm-mutTNF-R1 Mφ, and tm-mutTNF-R2 Mφ were stained with solTNFR1- or solTNFR2-Fc chimera that was labeled with PE-conjugated Fab fragment of anti-human Fc antibody. Shaded histograms show non-stained cells. (b) Mean fluorescence intensity of each cells is shown. (c) Values in parenthesis indicate the relative intensity against non-treated cells in each cell line.

for TNFR2. In this report, we established macrophage cell lines expressing only tmTNF, and not solTNF, owing to the deletion of the first 12 amino acids (Δ1–12) of each TNF mutant. Although most studies have made use of the Δ1–12 TNF mutation for the investigation of tmTNF activity, the bioactivity of the resulting non-cleavable tmTNF is reported to be reduced compared to

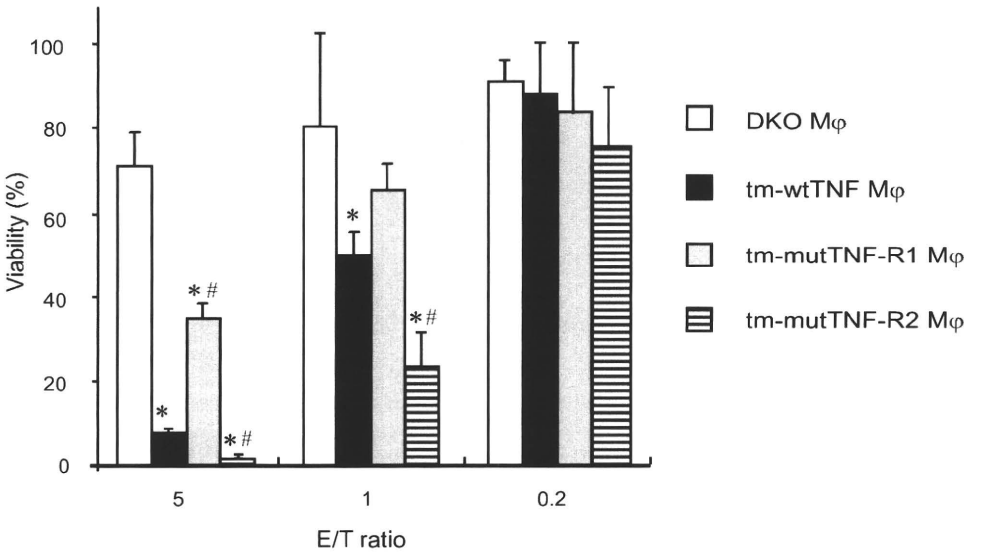

Fig. 5. tm-mutTNF-R2 Mφ induced death of hTNFR2/mFas-PA cells. hTNFR2/mFas-PA cells were co-incubated with paraformaldehyde-fixed DKO Mφ (open bars), tm-wtTNF Mφ (filled bards), tm-mutTNF-R1 Mφ (shaded bards), or tm-mutTNF-R2 Mφ (stiped bards) at an effector/target (E/T) ratio of 5:1, 1:1, or 0.2:1 in the presence of cycloheximide (1 μg/ml). After 48 h, cell viability was measured by the WST-8 Assay. Data were expressed as mean values ± SD of triplicate measurements and analyzed by one-way ANOVA (Dunnett's test). $^{*}p < 0.05$: compared to DKO Mφ, $^{\#}p < 0.05$: compared to tm-wtTNF Mφ.

wild-type tmTNF, whereas a tmTNF mutant containing a Δ1–9 K11E mutation exhibited normal cell-surface expression and a bioactivity similar to the wild-type [22]. Therefore, use of this latter deletion backbone may allow greater TNFR-selectivity in Mφ engineered to express tm-mutTNF-R2, and may generate superior TNFR-selective tmTNF-expressing cells.

As described earlier, tmTNF and solTNF have distinct roles or functions in normal and pathological conditions [8]. Furthermore, it is also believed that TNFR2 can only be fully activated by tmTNF [23]. Although the mechanisms underlying these effects are poorly understood, the half lives of the individual ligand/receptor complexes may contribute to the differential activity of tmTNF and solTNF [23]. Krippner-Heidenreich et al. reported that the dissociation rate constant of the cell surface binding of tmTNF to TNFR2 is much lower than that of the binding of solTNF to the same receptor, indicating that tmTNF dissociates much less readily from TNFR2 [24]. Thus, the bioactivity imparted by the interaction of the ligand/receptor pair is dependent upon various binding parameters (binding affinity, association or dissociation rate constant). We have shown here that tm-mutTNF-R2 Mφ exhibit greater cytotoxicity on hTNFR2/mFas-PA cells than do tm-wtTNF Mφ, whereas the cytotoxicity of sol-mutTNF-R2 was lower than that of sol-wtTNF. We assume that the dissociation rate constant of the binding of mutTNF-R2 to immobilized TNFR2 or TNFR2 on the cell surface might be reduced to a level similar to that of tm-wtTNF Mφ upon conversion of the soluble form to the transmembrane form. As such, the threefold higher association rate constant of the interaction of TNFR2 with sol-mutTNF-R2 than that of TNFR2 with sol-wtTNF (Table 1) might explain the strong bioactivity on hTNFR2/mFas-PA cells.

The affinity between a ligand and its receptor is determined by an equilibrium between the rates of association and dissociation, and is determined inherently. Therefore, expression of sol-mutTNFs with selectivity for each TNFR as the corresponding tmTNF forms on the cell surface, may alter the selectivity for the TNFRs. We plan to carry out more detailed analyses of the variant tmTNFs, such as measurement of their expression, their precise affinity for TNFR1 or R2, and their activity mediated through binding and signaling through TNFR1. Eventually, these tmTNFs, tm-mutTNF-R1 and R2 Mφ may prove useful for functional analysis or signal analysis of TNF receptors.

Acknowledgments

This study was supported in part by some Grants-in-Aid for Scientific Research from the Ministry of Education, Culture, Sports, Science and Technology of Japan, and in part by some Grants-in-Aid for Scientific Research from Japan Society for the Promotion of Science (JSPS). And this study was also supported in part by some Health Labour Sciences Research Grants from the Ministry of Health, Labor and Welfare of Japan, and in part by Health Sciences Research Grants for Research on Publicly Essential Drugs and Medical Devices from the Japan Health Sciences Foundation, in part by The Nagai Foundation Tokyo.

References

[1] Aggarwal BB. Signalling pathways of the TNF superfamily: a double-edged sword. Nat Rev Immunol 2003;3:745–56.
[2] Beutler B. Autoimmunity and apoptosis: the Crohn's connection. Immunity 2001;15:5–14.
[3] Feldmann M, Maini RN. Anti-TNF alpha therapy of rheumatoid arthritis: what have we learned? Annu Rev Immunol 2001;19:163–96.
[4] Feldmann M. Development of anti-TNF therapy for rheumatoid arthritis. Nat Rev Immunol 2002;2:364–71.
[5] Kriegler M, Perez C, DeFay K, Albert I, Lu SD. A novel form of TNF/cachectin is a cell surface cytotoxic transmembrane protein: ramifications for the complex physiology of TNF. Cell 1988;53:45–53.
[6] Tang P, Hung MC, Klostergaard J. Human pro-tumor necrosis factor is a homotrimer. Biochemistry 1996;35:8216–25.
[7] Black RA, Rauch CT, Kozlosky CJ, Peschon JJ, Slack JL, Wolfson MF, et al. A metalloproteinase disintegrin that releases tumour-necrosis factor-alpha from cells. Nature 1997;385:729–33.
[8] Ruuls SR, Hoek RM, Ngo VN, McNeil T, Lucian LA, Janatpour MJ, et al. Membrane-bound TNF supports secondary lymphoid organ structure but is subservient to secreted TNF in driving autoimmune inflammation. Immunity 2001;15:533–43.
[9] Mueller C, Corazza N, Trachsel-Loseth S, Eugster HP, Buhler-Jungo M, Brunner T, et al. Noncleavable transmembrane mouse tumor necrosis factor-alpha (TNFalpha) mediates effects distinct from those of wild-type TNFalpha in vitro and in vivo. J Biol Chem 1999;274:38112–8.
[10] Olleros ML, Guler R, Vesin D, Parapanov R, Marchal G, Martinez-Soria E, et al. Contribution of transmembrane tumor necrosis factor to host defense against Mycobacterium bovis bacillus Calmette-guerin and Mycobacterium tuberculosis infections. Am J Pathol 2005;166:1109–20.
[11] Saunders BM, Tran S, Ruuls S, Sedgwick JD, Briscoe H, Britton WJ. Transmembrane TNF is sufficient to initiate cell migration and granuloma formation and provide acute, but not long-term, control of Mycobacterium tuberculosis infection. J Immunol 2005;174:4852–9.

[12] Torres D, Janot L, Quesniaux VF, Grivennikov SI, Maillet I, Sedgwick JD. Membrane tumor necrosis factor confers partial protection to Listeria infection. Am J Pathol 2005;167:1677–87.
[13] Aggarwal BB, Eessalu TE, Hass PE. Characterization of receptors for human tumour necrosis factor and their regulation by gamma-interferon. Nature 1985;318:665–7.
[14] Micheau O, Tschopp J. Induction of TNF receptor I-mediated apoptosis via two sequential signaling complexes. Cell 2003;114:181–90.
[15] Perez C, Albert I, DeFay K, Zachariades N, Gooding L, Kriegler M. A nonsecretable cell surface mutant of tumor necrosis factor (TNF) kills by cell-to-cell contact. Cell 1990;63:251–8.
[16] Bryde S, Grunwald I, Hammer A, Krippner-Heidenreich A, Schiestel T, Brunner H, et al. Tumor necrosis factor (TNF)-functionalized nanostructured particles for the stimulation of membrane TNF-specific cell responses. Bioconjug Chem 2005;16:1459–67.
[17] Shibata H, Yoshioka Y, Ohkawa A, Minowa K, Mukai Y, Abe Y, et al. Creation and X-ray structure analysis of the tumor necrosis factor receptor-1-selective mutant of a tumor necrosis factor-alpha antagonist. J Biol Chem 2008;283:998–1007.
[18] Mukai Y, Shibata H, Nakamura T, Yoshioka Y, Abe Y, Nomura T, et al. Structure-function relationship of tumor necrosis factor (TNF) and its receptor interaction based on 3D structural analysis of a fully active TNFR1-selective TNF mutant. J Mol Biol 2009;385:1221–9.
[19] Abe Y, Yoshikawa T, Kamada H, Shibata H, Nomura T, Minowa K, et al. Simple and highly sensitive assay system for TNFR2-mediated soluble- and transmembrane-TNF activity. J Immunol Methods 2008;335:71–8.
[20] Katayama K, Wada K, Miyoshi H, Ohashi K, Tachibana M, Furuki R, et al. RNA interfering approach for clarifying the PPARgamma pathway using lentiviral vector expressing short hairpin RNA. FEBS Lett 2004;560:178–82.
[21] Miyoshi H, Smith KA, Mosier DE, Verma IM, Torbett BE. Transduction of human CD34+ cells that mediate long-term engraftment of NOD/SCID mice by HIV vectors. Science 1999;283:682–6.
[22] Decoster E, Vanhaesebroeck B, Vandenabeele P, Grooten J, Fiers W. Generation and biological characterization of membrane-bound, uncleavable murine tumor necrosis factor. J Biol Chem 1995;270:18473–8.
[23] Grell M, Douni E, Wajant H, Lohden M, Clauss M, Maxeiner B, et al. The transmembrane form of tumor necrosis factor is the prime activating ligand of the 80 kDa tumor necrosis factor receptor. Cell 1995;83:793–802.
[24] Krippner-Heidenreich A, Tubing F, Bryde S, Willi S, Zimmermann G, Scheurich P. Control of receptor-induced signaling complex formation by the kinetics of ligand/receptor interaction. J Biol Chem 2002;277:44155–63.

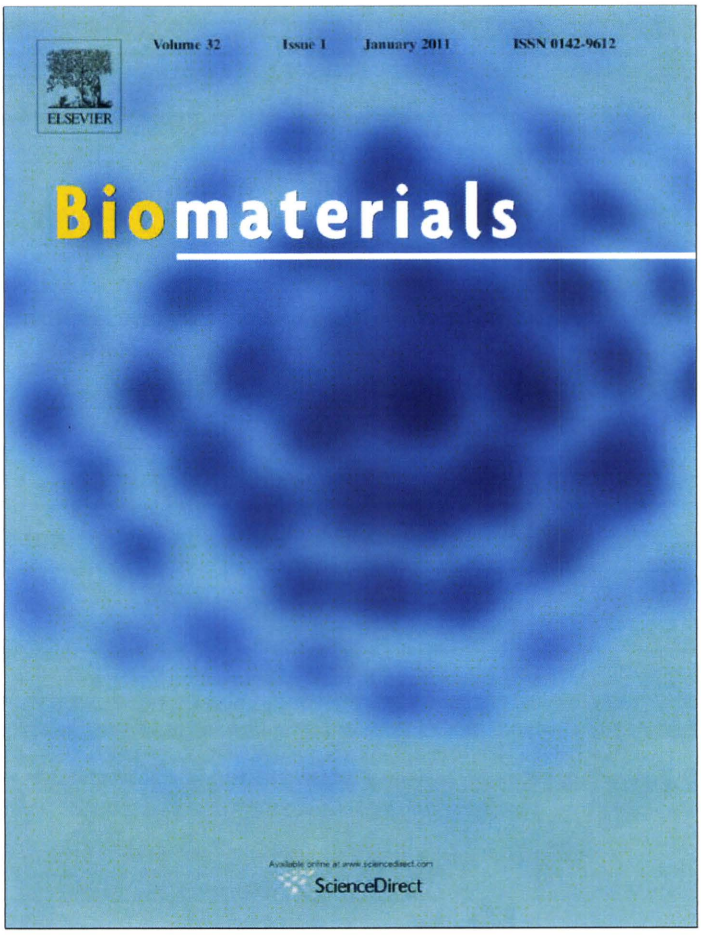

Biomaterials 32 (2011) 162–169

Contents lists available at ScienceDirect

Biomaterials

journal homepage: www.elsevier.com/locate/biomaterials

Development of an antibody proteomics system using a phage antibody library for efficient screening of biomarker proteins

Sunao Imai [a,1], Kazuya Nagano [a,1], Yasunobu Yoshida [a], Takayuki Okamura [a], Takuya Yamashita [a,b], Yasuhiro Abe [a], Tomoaki Yoshikawa [a,b], Yasuo Yoshioka [a,b,c], Haruhiko Kamada [a,c], Yohei Mukai [a,b], Shinsaku Nakagawa [b,c], Yasuo Tsutsumi [a,b,c], Shin-ichi Tsunoda [a,b,c,*]

[a] Laboratory of Biopharmaceutical Research, National Institute of Biomedical Innovation, 7-6-8 Saito-Asagi, Ibaraki, Osaka 567-0085, Japan
[b] Graduate School of Pharmaceutical Sciences, Osaka University, 1-6 Yamadaoka, Suita, Osaka 565-0871, Japan
[c] The Center of Advanced Medical Engineering and informatics, Osaka University, 1-6 Yamadaoka, Suita, Osaka 565-0871, Japan

ARTICLE INFO

Article history:
Received 27 August 2010
Accepted 14 September 2010
Available online 8 October 2010

Keywords:
Protein
Image analysis
Immunochemistry
Molecular biology
Antibody
Cancer

ABSTRACT

Proteomics-based analysis is currently the most promising approach for identifying biomarker proteins for use in drug development. However, many candidate biomarker proteins that are over- or under-expressed in diseased tissues are found by such a procedure. Thus, establishment of an efficient method for screening and validating the more valuable targets is urgently required. Here, we describe the development of an "antibody proteomics system" that facilitates the screening of biomarker proteins from many candidates by rapid preparation of cross-reacting antibodies using phage antibody library technology. Using two-dimensional differential in-gel electrophoresis analysis, 16 over-expressed proteins from breast cancer cells were identified. Specifically, proteins were recovered from the gel pieces and a portion of each sample was used for mass spectrometry analysis. The remainder was immobilized onto a nitrocellulose membrane for antibody-expressing phage enrichment and selection. Using this procedure, antibody-expressing phages against each protein were successfully isolated within two weeks. The expression profiles of the identified proteins were then acquired by immunostaining of breast tumor tissue microarrays with the antibody-expressing phages. Using this approach, expression of Eph receptor A10, TRAIL-R2 and Cytokeratin 8 in breast tumor tissues were successfully validated.

These results demonstrate the antibody proteomics system is an efficient method for screening tumor-related biomarker proteins.

1. Introduction

Proteomics-based analysis is the most promising approach for identifying tumor-related biomarker proteins used in the drug development process [1–3]. The technological development of proteomics to seek and identify differentially expressed proteins in disease samples is expanding rapidly. However, in spite of the identification of many candidate biomarkers, the number of biomarker proteins successfully applied to drug development has been limited. The main difficulty is the lack of a methodology to comprehensively analyze the expression or function of many candidate proteins and to efficiently select potential biomarker proteins of interest. To circumvent this problem, an improved technology to efficiently screen the truly valuable proteins from a large number of candidates is desirable.

Monoclonal antibodies are extremely useful tools for the functional and distributional analysis of proteins [4–6]. For example, they can be applied to the specific detection and study of proteins through various techniques including ELISA, Western blotting, fluorescent imaging and tissue microarray analysis (TMA). Of all these techniques, TMA is particularly valuable because it enables the analysis of clinical expression profiles of antigens from many clinical samples [7–11]. However, the common hybridoma-based antibody production is a laborious and time-consuming method. Thus, it is impractical to create antibodies against many differentially expressed proteins identified by proteomics technologies, such as two-dimensional differential in-gel electrophoresis (2D-DIGE) [12–15]. Furthermore, a relatively large amount of antigen (several milligrams) is necessary to produce an antibody (i.e., immunization of animals or screening of positive clones). The

* Corresponding author. Laboratory of Biopharmaceutical Research, National Institute of Biomedical Innovation, 7-6-8 Saito-Asagi, Ibaraki, Osaka 567-0085, Japan. Tel.: +81 72 641 9814; fax: +81 72 641 9817.
E-mail address: tsunoda@nibio.go.jp (S.-i. Tsunoda).
[1] These authors contributed equally to the work.

0142-9612/$ – see front matter © 2010 Elsevier Ltd. All rights reserved.
doi:10.1016/j.biomaterials.2010.09.030

production of protein on this scale often requires engineering the corresponding gene for heterologous expression, which may require some time to optimize. In this respect, phage antibody library technology is able to construct a large repertoire protein or peptide consisting of hundreds of millions of molecules. Monoclonal antibodies against target antigens are then rapidly obtained from the phage libraries displaying single chain fragment variable (scFv) antibodies *in vitro* [16–21].

However, the amount of protein in spots detected by 2D-DIGE analysis is generally very small (hundreds of nanograms). Therefore, a technology for generating monoclonal antibodies from such small amounts of antigen needs to be developed. There are no reports that describe the successful isolation of antibodies against small amounts of proteins obtained from differential proteome analysis.

Here, we report the establishment of a method for the efficient isolation of scFv antibody-expressing phages from a small amount of protein antigen prepared *via* 2D-DIGE spots using a high quality non-immune mouse scFv phage library [22]. We also describe an efficient method for screening and validating tumor-related biomarker proteins of interest from a number of differentially expressed proteins by expression profiling using TMA and scFv antibody-expressing phages.

2. Materials and methods

2.1. Non-immune mouse scFv phage library

Construction of the improved non-immune murine scFv phage library has been described previously [22]. The phage library was prepared from a TG1 glycerol stock containing the scFv gene library.

2.2. Affinity panning using BIAcore® and nitrocellulose membrane

Three different amounts (5000 ng, 50 ng or 0.5 ng) of KDR-Fc chimera (R&D systems Inc., Minneapolis, MN) or a portion of the proteins (1–5 ng) extracted from 2D-DIGE spots were immobilized on a BIAcore sensor chip CM3® (BIAcore, Uppsala, Sweden) or on a nitrocellulose membrane. BIAcore-based panning has been described previously [22]. Membrane-based panning was performed using the Bio-Dot Microfiltration Apparatus (Bio-Rad Laboratories, Hercules, CA). The membrane was incubated with blocking solution (10% skimmed milk, 25% glycerol) for 2 h and then washed twice with 0.1% TBST (Tris-buffered saline containing 0.1% Tween 20). The model phage library (anti-KDR scFv antibody-expressing phages: wild type phage = 1: 100) or the non-immune scFv phage library was pre-incubated with 90% blocking solution at 4 °C for 1 h and then applied to each well. After 2–3 h incubation, the apparatus was washed ten times with TBST. Bound scFv antibody-expressing phages were then eluted with 100 mM triethylamine. The eluted phages were incubated in log phase *E. coli* TG1 cells and glycerol-stocks prepared for further repeat panning cycles. Phage titer was measured by counting the number of infected colony cells on Petrifilm (3M Co., St. Paul, MN).

2.3. Colony direct PCR

After the panning, colonies of phage-infected TG1 were picked up at random as PCR templates. The gene inserts of 16 clones were amplified by PCR using the following primers: primer-156 (5′-CAACGTGAAAAAATTATTATTCGC-3′) and primer-158 (5′-GTAAATGA ATTTTCTGTATGAGG-3′), which anneal to the sequences of pCANTAB5E phagemid vector (GE Healthcare Biosciences AB, Uppsala, Sweden). The size of insert DNA sequence was analyzed by agarose gel electrophoresis.

2.4. Cell lines

Human mammary gland cell line 184A1 (American Type Culture Collection; ATCC, Manassas, VA) was maintained by MEGM Bullet Kit (Takara Bio, Shiga, JAPAN). Mammary gland-derived breast cancer cell line SKBR3 (ATCC) was maintained in McCoy's 5a plus 10% FBS. All cells were grown at 37 °C in a humidified incubator with 5% CO_2.

2.5. 2D-DIGE analysis

Cell lysates were prepared from human mammary gland cell line 184A1 and mammary gland-derived breast cancer cell line SKBR3, and then solubilized with 7 M urea, 2 M thiourea, 4% CHAPS and 10 mM Tris–HCl (pH 8.5). The lysates were labeled at the ratio 50 μg protein: 400 pmol Cy3 or Cy5 protein labeling dye (GE Healthcare Biosciences AB) in dimethylformamide according to the manufacture's protocol. For first dimension separation, the labeled samples (each 50 μg) were combined and mixed with rehydration buffer (7 M urea, 2 M thiourea, 4% CHAPS, 2% DTT, 2% Pharmalyte (GE Healthcare Biosciences AB)) and applied to a 24-cm immobilized pH gradient gel strip (IPG-strip pH 5–6 NL). The samples for the spot-picking gel were prepared without labelling by Cy-dyes. For the second dimension separation, the IPG-strips were applied to SDS-PAGE gels (10% polyacrylamide and 2.7% N,N′-diallyltartardiamide gels). After electrophoresis, the gels were scanned with a laser fluoroimager (Typhoon Trio, GE Healthcare Biosciences AB). The spot-picking gel was scanned after staining with Flamingo solution (Bio-Rad). Quantitative analysis of protein spots was carried out with Decyder-DIA software (GE Healthcare Biosciences AB). For the antigen spots of interest, spots of 1 × 1 mm in size were picked using an Ettan Spot Picker (GE Healthcare Biosciences AB). Proteins were extracted by solubilizing the picked gel pieces using 88 mM sodium periodide. Protein volumes were determined by BSA standard in Colloid Gold Total Protein staining (Bio-Rad).

2.6. In-gel tryptic digestion

Spots of 1 mm × 1 mm in size were picked using an Ettan Spot Picker and digested with trypsin as described below. The gel pieces were then destained with 50% acetonitrile/50 mM NH_4HCO_3 for 20 min twice, dehydrated with 75% acetonitrile for 20 min, and then dried using a centrifugal concentrator. Next, 5 μl of 20 μl/ml trypsin (Promega, Madison, WI) solution was added to each gel piece and incubated for 16 h at 37 °C. Three solutions were used to extract the resulting peptide mixtures from the gel pieces. First, 50 μl of 50% (v/v) acetonitrile in 1% (v/v) aqueous trifluoroacetic acid (TFA) was added to the gel pieces, which were then sonicated for 5 min. Next, we collected the solution and added 80% (v/v) acetonitrile in 0.2% TFA. Finally, 100% acetonitrile was added for the last extraction. The peptides were dried and then resuspended in 10 μl of 0.1% TFA before being cleaned using ZipTip^{TM} μC_{18} pipette tips (Millipore, Billerica, MA). The tips were wetted with three washes in 50% acetonitrile and equilibrated with three washes in 0.1% TFA, then the peptides were aspirated 10 times to ensure binding to the column. The column and peptides were washed three times in 0.1% TFA before being eluted in 1 μl of 80% acetonitrile/0.2% TFA.

2.7. Mass spectrometry (MS) and database search

The tryptic digests (0.6 μl) were mixed with 0.6 μl α-cyano-4-hydroxy-trans-cinnamic acid saturated in a 0.1% TFA and acetonitrile solution (1:1vol/vol). Each mixture was deposited onto a well of a 96-well target plate and then analyzed by matrix-assisted laser desorption ionization time-of-flight mass spectrometry (MALDI-TOF/MS; autoflexII, Bruker Daltonics, Billerica, WI) in the Reflectron mode. The mass axis was adjusted with calibration peptide (BRUKER DALTNICS) peaks (M/z 1047.19, 1296.68, or 2465.19) as lock masses. Bioinformatic databases were searched to identify the proteins based on the tryptic fragment sizes. The Mascot search engine (http://www.matrixscience.com) was initially used to query the entire theoretical tryptic peptide as well as SwissProt (http://www.expasy.org/, a public domain database provided by the Swiss Institute of Bioinformatics, Geneva, Switzerland). The search query assumed the following: (i) the peptides were monoisotopic (ii) methionine residues may be oxidized (iii) all cysteines are modified with iodoacetamide.

2.8. Phage ELISA using nitrocellulose membrane

Phage ELISA using scFv antibody-expressing phages was performed as previously described [22]. Briefly, phage-infected TG1 clones were picked, monocloned in a Bio-Dot Microfiltration Apparatus and scFv antibody-expressing phages propagated. The supernatants containing scFv antibody-expressing phages were incubated with immobilized proteins (~1 ng) extracted from 2D-DIGE spots. scFv antibody-expressing phages bound to 2D-DIGE spots were visualized using HRP-conjugated anti-M13 monoclonal antibody (GE Healthcare Biosciences AB).

2.9. Immunohistochemical staining using scFv antibody-expressing phages

Human breast cancer and normal TMA (Super Bio Chips, Seoul, South Korea & Biomax, Rockville, MD) were deparaffinated in xylene and rehydrated in a graded series of ethanol. Heat-induced epitope retrieval was performed in while keeping Target Retrieval Solution pH 9 (Dako, Glostrup, Denmark) temperature following the manufacturer's instructions. Heat-induced epitope retrieval was performed while maintaining the Target Retrieval Solution pH 9 (Dako) at the desired temperature according to the manufacturer's instructions. After heat-induced epitope retrieval treatment, endogenous peroxidase was blocked with 0.3% H_2O_2 in TBS for 5 min followed by washing twice in TBS. TMA were incubated with 5% BSA blocking solution for 15 min. The slides were then incubated with the primary scFv antibody-expressing phages (10^{12} CFU/ml) for 60 min. After washing three times with 0.05% TBST, each series of sections was incubated for 30 min with ENVISION + Dual Link (Dako), washed three times in TBST. The reaction products were rinsed twice with TBST, and then developed in liquid 3,3′-diaminobenzidine (Dako) for 3 min. After the development, sections were washed twice with distilled water, lightly

counterstained with Mayer's hematoxylin, dehydrated, cleared, and mounted with resinous mounting medium. All procedures were performed using AutoStainer (Dako).

2.10. TMA Immunohistochemistry scoring

The optimized staining condition for breast tumor tissue microarray was determined based on the coexistence of both positive and negative cells in the same tissue sample. Signals were considered positive when reaction products were localized in the expected cellular component. The criteria for the staining were scored as follows: distribution score was scored as 0 (0%), 1 (1–50%), and 2 (51–100%) to indicate the percentage of positive cells in all tumor cells present in one tissue. The intensity of the signal (intensity score) was scored as 0 (no signal), 1 (weak), 2 (moderate) or 3 (marked). The total of the distribution score and intensity score was then summed into a total score (TS) of TS0 (sum = 0), TS1 (sum = 2), TS2 (sum = 3), and TS3 (sum = 4–5). Throughout this study, TS0 or TS1 was regarded as negative, whereas TS2 or TS3 was regarded as positive. Statview software was used in statistical analysis.

3. Results

3.1. Optimization of panning methods

To establish a method for the efficient isolation of antibodies against a small amount of protein antigen (nanogram-order or less) prepared from 2D-DIGE spots, 5000 ng, 50 ng or 0.5 ng of recombinant KDR proteins were first immobilized on a BIAcore sensor chip CM3® or on a nitrocellulose membrane using the Bio-Dot Microfiltration Apparatus®. Isolation of antibodies was assessed using a model phage library (anti-KDR scFv antibody-expressing phages: wild type phage = 1: 100) (Fig. 1). Enrichment of the desired clones in the output library was evaluated by analyzing the gene inserts of randomly-picked phage-infected TG1 cells by colony direct PCR. In the method using BIAcore®, enrichment was observed when 5000 ng of KDR was used for immobilization. By contrast, Membrane-based panning led to the successful enrichment of anti-KDR scFv antibodies from only 0.5 ng of KDR. These results demonstrated that membrane-based panning was suitable for the isolation of antibodies from very small amounts of antigen extracted from 2D-DIGE spot gel pieces.

3.2. 2D-DIGE analysis and identification of differentially expressed proteins

To identify breast tumor-related biomarker proteins and isolate monoclonal antibodies against them, we performed 2D-DIGE using breast cancer cell lines SKBR3 and normal breast cell lines 184A1 (Fig. 2). Quantitative analysis showed that 21 spots displayed increased or decreased expression levels in the cancer cell line compared with the normal cell line. MALDI-TOF/MS analysis of the spots subsequently identified 16 different proteins (Table 1).

3.3. Isolation of antibodies against each 2D-DIGE spot from the non-immune scFv phage library

The amount of protein extracted from the gel pieces ranged from several tens of nanogram to a few micrograms (Table 1). Because the membrane-based panning method facilitates the isolation of antibodies from 0.5 ng of protein (Fig. 1), we reasoned that this method could be used to isolate antibodies from the small amounts of proteins extracted from 2D-DIGE spot gel pieces. Thus a portion of the extracted proteins were immobilized onto nitrocellulose membranes by means of a Bio-Dot Microfiltration Apparatus, and membrane-based panning was performed using the non-immune scFv phage library [22] (Table 2). The results from this panning showed that the output/input ratio of phage titer (titer of the recovered phage library after the panning/titer of phage library before the panning) after the fourth round of panning against all spots increased approximately 20-fold–4000-fold in comparison to that obtained from the first round of panning. This elevated output/input ratio indicated the enrichment of the antigen-binding scFv antibody clones. To isolate monoclonal scFv antibodies to each spot, a total of 60 clones were randomly picked from the 4th panning output phage library and binding of the monoclonal scFv antibody-expressing phages to each antigen was tested by phage ELISA. As a result, several scFv antibody clones binding to each of the 16 antigens were isolated (Table 2). The antigenic specificity of isolated scFv antibodies was investigated by dot blot using various proteins as antigens. Some of the isolated scFv antibodies bound specifically to the antigen protein, but not to the His-tagged caspase-8, His-tagged importin-β, tumor necrosis factor receptor 1 (TNFR1)-Fc-chimera and KDR-Fc-chimera (data not shown). These results indicated the successful isolation of each spot-specific scFv antibody-expressing phages after only two weeks.

3.4. TMA analysis

The next stage in the process was to select the most valuable breast tumor-related biomarker proteins from a large number of

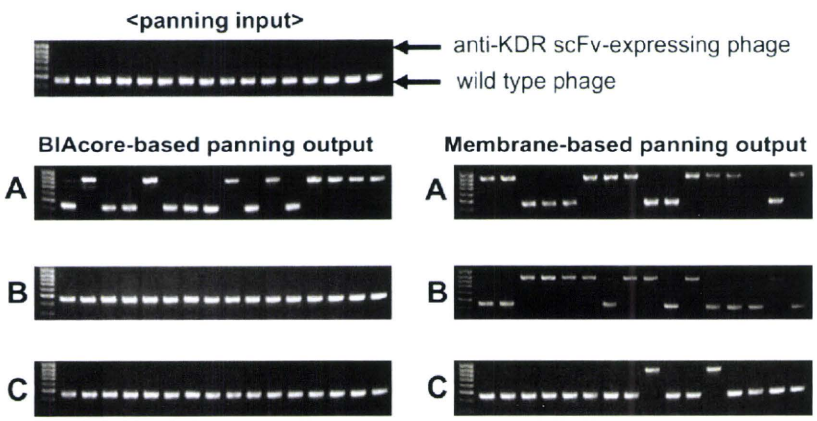

Fig. 1. Optimization of panning methods to isolate monoclonal antibodies from a very small amount of antigen. Model panning was performed using the BIAcore® or nitrocellulose membrane. The model library (anti-KDR scFv phage : wild type phage = 1: 100) was incubated with KDR ((A) 5000 ng, (B) 50 ng, (C) 0.5 ng) immobilized on a sensor chip or nitrocellulose membrane. The BIAcore-based panning method has been previously described [22]. After the binding step, the nitrocellulose membrane was washed ten times with TBST. The bound scFv antibody-expressing phages were eluted with triethylamine. The eluted scFv antibody-expressing phages were then incubated in log phase TG1 cells and individual TG1 clones were picked at random. Inserts of 16 phage clones were amplified by PCR. The gene sizes of inserts were analyzed by agarose gel electrophoresis.

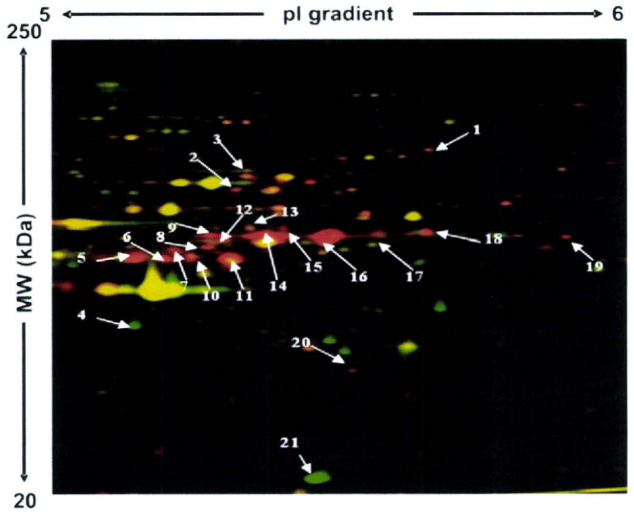

Fig. 2. 2D-DIGE image of fluorescently labeled proteins from SKBR3 and 184A cell. Breast cancer cell line (SKBR3) and normal breast cell line (184A1) were labeled using cy3 and cy5, respectively. The protein samples were then subjected to 2D electrophoresis. Spots that were over- and under-expressed in mammary cancer cells relative to normal cells were colored red and green, respectively. Yellow color spots show no change in expression.

identified candidate proteins. To this end, we immunostained TMA slides with 189 cases of breast tumors and 15 cases of normal breast specimens using the isolated spot-specific scFv antibody-expressing phages and screened the promising candidate biomarker proteins in terms of the expression profile in breast tumor tissues and normal tissues (Table 3). The result of the expression profile analysis showed that SPATA5, beta-actin variant, FLJ31438, PAK65, XRN1 and Jerky protein homolog-like were not expressed in normal and breast cancer tissue at all. By contrast, TRAIL-R2, Cytokeratin 8 and Eph receptor A10 were highly and specifically expressed (Fig. 3) in 63, 73 and 49% of breast tumor cases respectively, while the existing-breast cancer marker, Her-2, was expressed in 28% of breast tumor cases (Table 3). Thus, the relationship between the expression of each antigen and the Her-2 expression profile was analyzed. The level of expression of TRAIL-R2, Cytokeratin 8 and Eph receptor A10 in Her-2 positive cases were 77, 77 and 62%, and in Her-2 negative cases were 57, 67 and 44%, respectively (Table 4). Furthermore, the relationship between the expression of each antigen and clinical stage was analyzed in 187 of the 189 cases where all the clinical data was available. The level of expression of Cytokeratin 8 and Eph receptor A10 increased with progression of clinical symptoms (Table 5).

Table 1
Identification of 2D-DIGE spots by MALDI-TOF/MS.

Spot	Protein name	Accession number	MW (kDa)	pI	Protein volume (ng)	Expression ratio [cancer/normal] (fold)
#1	splicing factor YT521-B	Q96MU7	85	5.9	119	6
#2	IkappaBR	Q96HA7	63	5.5	104	6
#3	SPATA5	C9JT97	76	5.6	94	7
#4	skin aspartic protease	Q53RT3	37	5.3	610	0.1
#5	beta actin variant	P60709	42	5.3	99	15
#6	TRAIL-R2	O14763	48	5.4	100	18
#7	Cytokeratin-18	P05783	48	5.3	99	12
#8	TRAIL-R2	O14763	48	5.4	95	16
#9	RREB1	Q92766	52	5.3	109	10
#10	Cytokeratin-7	P08729	51	5.4	126	23
#11	Cytokeratin-18	P05783	48	5.3	497	13
#12	Cytokeratin-7	P08729	51	5.4	122	24
#13	FLJ31438	Q96N41	53	5.5	126	35
#14	Cytokeratin-7	P08729	51	5.4	406	36
#15	PAK65	Q13177	55	5.7	677	8
#16	Cytokeratin 8	P05787	54	5.5	694	32
#17	Cytokeratin 8	P05787	54	5.5	1143	72
#18	XRN1	Q8IZH2	54	5.8	353	8
#19	Jerky protein homolog-like	Q9Y4A0	51	6.0	130	22
#20	Eph receptor A10	Q5JZY3	32	5.7	119	9
#21	Glutathione S-transferase P	P09211	23	5.4	119	0.02

Table 2
Enrichment and isolation of antibodies to 2D-DIGE spots from non-immune libraries.

Spot	Protein name	Output/Input Ratio ($\times 10^{-7}$)/round				The number of isolated mAb.
		1st	2nd	3rd	4th	
#1	splicing factor YT521-B	6	7	16	480	4
#2	IkappaBR	6	7	15	500	3
#3	SPATA5	5	6	32	860	2
#4	skin aspartic protease	5	6	5	24	1
#5	beta actin variant	7	11	17	480	1
#6	TRAIL-R2	6	7	25	420	5
#7	Cytokeratin 18	5	11	62	260	4
#8	TRAIL-R2	5	27	41	1500	5
#9	RREB1	8	9	14	370	7
#10	Cytokeratin 7	6	7	3	2200	5
#11	Cytokeratin 18	6	8	15	84	2
#12	Cytokeratin 7	10	11	13	94	2
#13	FLJ31438	7	9	32	80	6
#14	Cytokeratin 7	4	7	46	280	5
#15	PAK65	7	11	51	580	9
#16	Cytokeratin 8	8	7	16	4100	6
#17	Cytokeratin 8	5	12	33	240	2
#18	XRN1	6	20	18	200	1
#19	Jerky protein homolog-like	7	10	49	940	3
#20	Eph receptor A10	8	6	57	3000	2
#21	Glutathione S-transferase P	7	8	110	1900	2

4. Discussion

Here, we aimed to develop a method of efficiently screening tumor-related biomarker proteins by proteome analysis. In

Table 3
Positive rate of identified proteins in breast cancer and normal breast tissues.

Protein name	Positive rate of antigens			
	Normal breast tissues		Breast cancer tissues	
Her-2	0/15	(0%)	53/189	(28%)
IkappaBR	3/15	(20%)	22/189	(12%)
SPATA5	0/15	(0%)	0/189	(0%)
beta actin variant	0/15	(0%)	0/189	(0%)
TRAIL-R2	0/15	(0%)	119/189	(63%)
RREB1	1/15	(7%)	83/189	(44%)
FLJ31438	0/15	(0%)	0/189	(0%)
PAK65	0/15	(0%)	0/189	(0%)
Cytokeratin 8	0/15	(0%)	137/189	(73%)
XRN1	0/15	(0%)	0/189	(0%)
Jerky protein homolog-like	0/15	(0%)	0/189	(0%)
Eph receptor A10	0/15	(0%)	93/189	(49%)

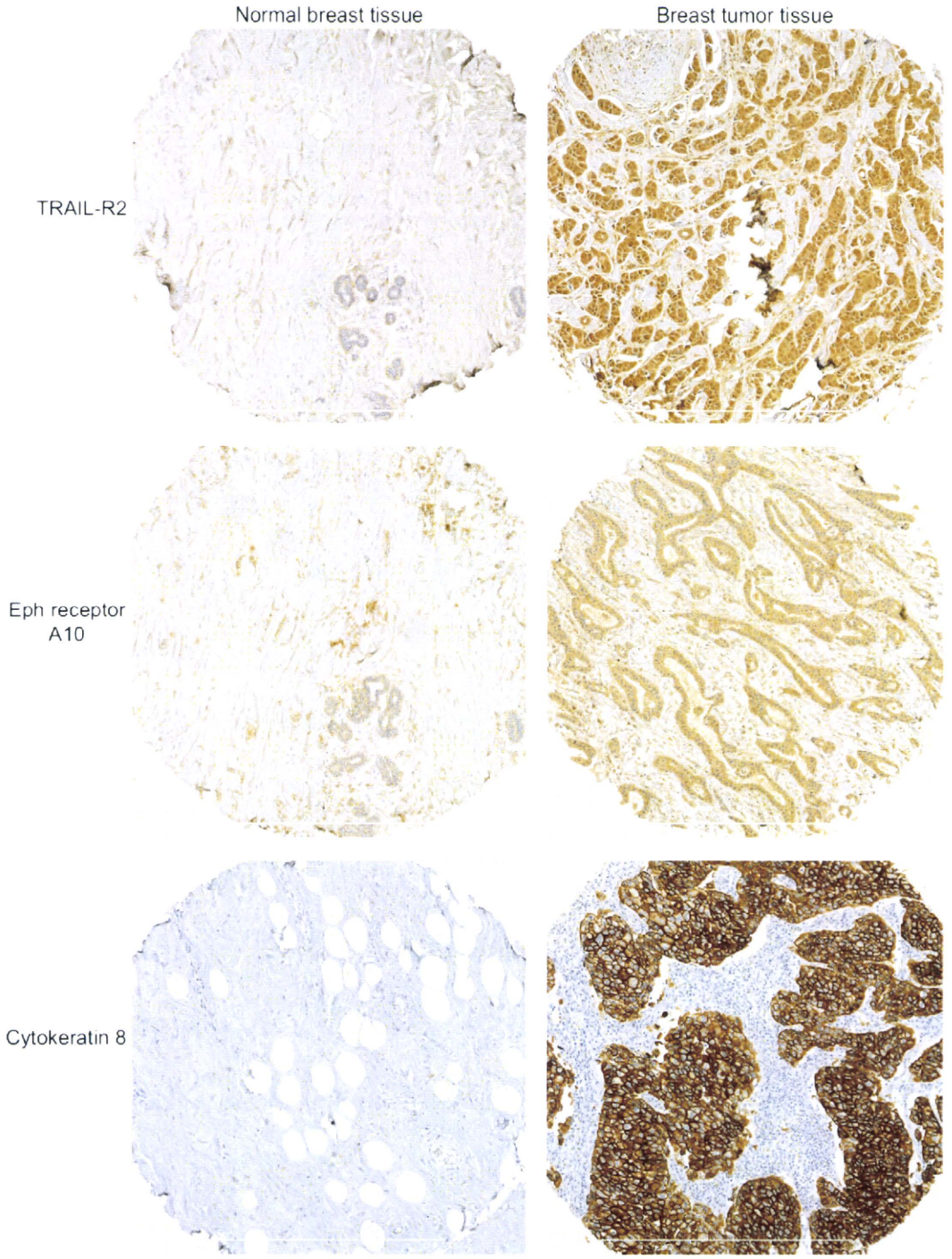

Fig. 3. Immunohistochemical staining of breast tumor and normal breast tissue microarray by scFv antibody-expressing phages. Typical images of breast cancer and normal breast tissue microarray stained by using scFv antibody-expressing phages to TRAIL-R2, Eph receptor A10 and Cytokeratin 8 are shown. Left panels are normal breast tissues and right panels are breast tumors. The tissue microarrays were counterstained by hematoxylin.

particular, we attempted to establish a means of isolating specific antibodies directly from small amounts of differentially expressed proteins obtained *via* 2D-DIGE analysis. To achieve this, we focused on a non-immune scFv phage library. Because the non-immune naïve scFv phage library has a huge repertoire of scFv on the surface of the phages, monoclonal antibodies to every antigen could be effectively isolated *in vitro*. Generally the diversity of the CDR3 domain, which is important for antigen-binding specificity, is estimated to be approximately twenty million [23]. Thus we reasoned that our previously constructed library, containing 2.4×10^9 scFv variants, has almost equal potential as the murine or human immune system [22]. Initially, in order to isolate monoclonal antibodies against very small amounts of antigen (hundreds of nanograms) recovered from the spots of 2D-DIGE analysis, we attempted to optimize the panning method using either a BIAcore® or nitrocellulose membrane. In the method using BIAcore®, the

Table 4
Positive rate of identified proteins in Her-2 positive and Her-2 negative cases.

Protein name	Positive rate of antigens in Her-2	
	Positive cases	Negative cases
TRAIL-R2	41/53 (77%)	78/136 (57%)
Cytokeratin 8	41/53 (77%)	91/136 (67%)
Eph receptor A10	33/53 (62%)	60/136 (44%)
TRAIL-R2 or Eph receptor A10	46/53 (87%)	100/136 (74%)

Table 5
Positive rate of identified proteins in clinical stage.

Protein name	Positive rate of antigens in clinical stage					
	Stage I		Stage II		Stage III	
Her-2	6/14	(43%)	17/87	(20%)	30/86	(35%)
TRAIL-R2	11/14	(79%)	51/87	(59%)	55/86	(64%)
Cytokeratin 8*	7/14	(50%)	58/87	(67%)	71/86	(83%)
Eph receptor A10*	4/14	(29%)	42/87	(48%)	47/86	(55%)

Man Whitney U test $^*P < 0.05$

enrichment of the desired clones was observed when immobilizing 5000 ng of KDR. By contrast, membrane-based panning led to the successful enrichment of clones from only 0.5 ng of KDR (Fig. 1). BIAcore-based panning has been recognized to be an effective method because the interaction of an antigen and a scFv antibody can be monitored in real time and the operation can be automated [24,25]. However, our results suggest that BIAcore® is inefficient for immobilizing very small amounts of antigen. This is because antigen immobilization using the BIAcore procedure requires a chemical coupling reaction with the surface of the sensor chip. In contrast, the membrane-based panning method is suitable for the isolation of antibodies against very small amounts of antigens. The suitability of this procedure when handling such small amounts of proteins presumably arises from the high efficiency of adsorption of antigens by the nitrocellulose membrane. These results show that monoclonal antibodies can be created from small amounts of proteins recovered from 2D-DIGE spots.

In breast cancer patients, the antibody targeting human epidermal growth factor receptor II (Her-2), is an effective drug [26,27]. However, because this receptor is over-expressed in only ~25% of breast cancer patients, anti-Her-2 antibody therapy is ineffective in ~75% of cases. Furthemore, approximately 30% of Her-2 over-expressed patients that received anti-Her-2 antibody therapy became tolerant [28–30]. Thus, we applied our antibody proteomics system to breast cancer samples for identification of the proteins to replace Her-2 as suitable therapeutic targets. Initially, 21 differentially expressed proteins between SKBR3 and 184A1 cells were found by 2D-DIGE analysis and 16 different proteins were identified by MALDI-TOF/MS. Four of the identified proteins were present in more than one spot i.e., TRAIL-R2 (spot 6, 8), Cytokeratin 18 (spot 7, 11), Cytokeratin 8 (spot 16, 17) and Cytokeratin 7 (spot 10, 12, 14). These proteins presumably display different pI and MW values due to posttranslational modification. Next, membrane-based panning against these spots was performed, and the output/input ratio of phage titer after the fourth round of panning increased from approximately 20-fold–4000-fold in comparison to that after the first round of panning. Moreover, we screened scFv antibody-expressing phages binding to each spot protein by phage ELISA and obtained each spot-specific scFv antibodies from all spots after approximately two weeks. Finally, it was necessary to select the most valuable proteins from a large number of differentially expressed proteins in breast cancer cells. Using the isolated spot-specific scFv antibody-expressing phages, we immunostained a TMA with 189 cases of breast cancer tissue and 15 samples of normal tissue. SPATA5, Beta actin, FLJ31438, PAK65 and XRN1 were not detected in either the tumor tissue or normal tissue. Thus, these proteins may have been derived from cell lines used in the

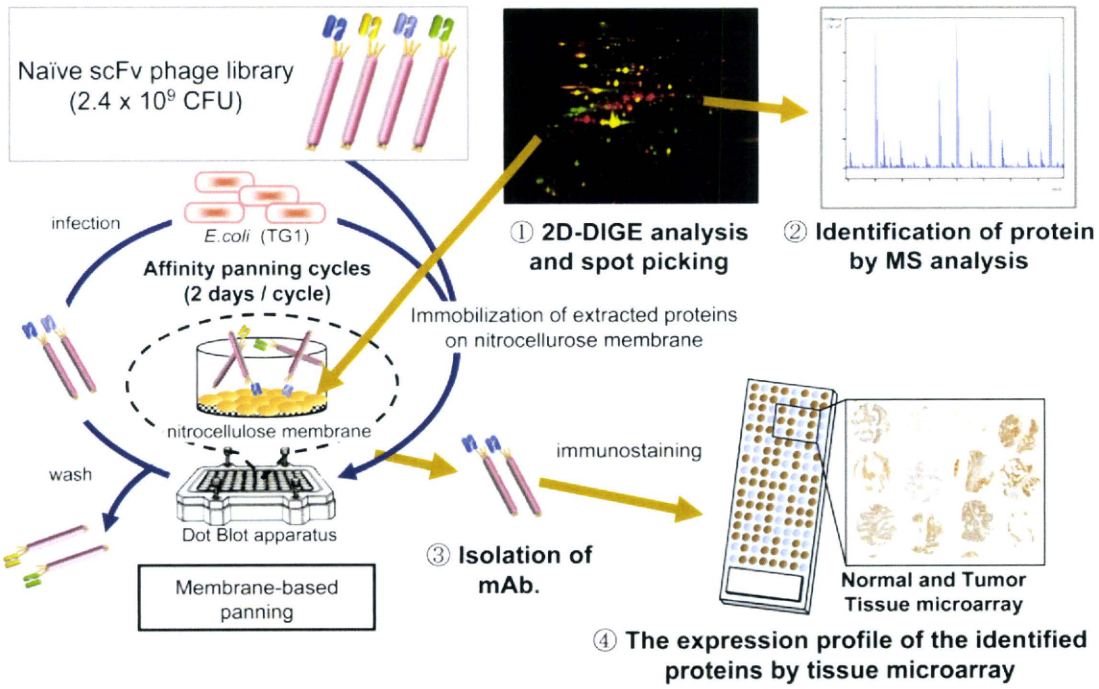

Fig. 4. Schematic illustration of the antibody proteomics system. Antibody proteomics system is an efficient method for screening tumor-related biomarker proteins. Because this system involves the direct isolation of monoclonal antibodies from 2D-DIGE spots without preparation of recombinant proteins, it enables the discovery and validation of tumor-related biomarker proteins by TMA analysis using the isolated scFv antibody-expressing phages.

proteome analysis or the antibodies against these proteins may not detect the antigen on formalin-fixed paraffin-embedded tissues. By contrast, TRAIL-R2, Cytokeratin 8 and Eph receptor A10 were specifically-expressed in over 40% of breast cancer tissues. We confirmed the immunohistochemical staining image generated by scFv antibody-expressing phages displayed a similar pattern to that generated by IgG type commercial antibody (data not shown). Interestingly, the expression rates of TRAIL-R2, Cytokeratin 8 and Eph receptor A10 were higher than the existing breast cancer marker, Her-2 (only about 25%). Moreover, the expression rates of TRAIL-R2 and Eph receptor A10 (cell membrane proteins) in Her-2 negative cases were over 40% and in Her-2 positive cases over 60%. This data indicates that TRAIL-R2 and Eph receptor A10 are promising alternative target candidates for anti-Her-2 antibody therapy ineffective patients, at least in terms of the expression profile. Further work is required to analyze the function of these proteins in more detail. Furthermore, by checking antigen expression profiles against clinical information, the expression rate of Cytokeratin 8 and Eph receptor A10 was found to have increased during progression of the clinical symptoms. These observations indicate that Cytokeratin 8 and Eph receptor A10 are promising diagnostic marker candidates for assessing the aggressiveness of breast cancer.

Recently, an anti-TRAIL-R2 antibody has been developed as an anticancer drug [31–33]. Moreover, Cytokeratin 8 has gained considerable attention as a cancer aggressiveness diagnostic marker [34–36]. These results demonstrate that this technology is able to select well-known drug-target markers (i.e., TRAIL-R2) and diagnostic markers (i.e., Cytokeratin 8) as well as unknown biomarker protein candidates (Eph receptor A10) from a large variety of differentially expressed proteins in cancer cells.

Our method employs a set of techniques for efficiently identifying biomarker candidates. Specifically, the method entails; 1) searching for differentially expressed proteins in disease samples, 2) identification of the proteins, 3) high throughput isolation of monoclonal antibodies against the proteins using a naïve scFv phage library, and 4) validation of the proteins by TMA analysis. This methodology is referred to as an "antibody proteomics system" (Fig. 4). We believe that the proteins identified using this approach will contribute to the drug development process. Indeed, the antibody proteomics system could become a platform technology for seeking tumor-related biomarker proteins by a proteomics-based approach.

5. Conclusions

In this study, we established the antibody proteomics system for efficiently screening and validating tumor-related biomarker proteins of interest by isolating specific antibodies directly from small amounts of proteins obtained *via* 2D-DIGE analysis. Applying this technique to the identification of breast tumor-related biomarker proteins, the expressions of Eph receptor A10, TRAIL-R2 and Cytokeratin 8 in breast tumor tissues were successfully validated from a large number of candidates. These results demonstrate that our original technology is an efficient and useful method for screening tumor-related biomarker proteins. Moreover, Eph receptor A10, TRAIL-R2 and Cytokeratin 8 identified in this study are promising breast tumor biomarkers for drug development.

Acknowledgement

We thank Dr. Junya Fukuoka, Department of Surgical Pathology, Toyama University Hospital, for valuable advice during our pathological analysis.

This study was supported in part by Grants-in-Aid for Scientific Research from the Ministry of Education, Culture, Sports, Science and Technology of Japan, and from the Japan Society for the Promotion of Science (JSPS). This study was also supported in part by Health Labour Sciences Research Grants from the Ministry of Health, Labor and Welfare of Japan, and by Health Sciences Research Grants for Research on Publicly Essential Drugs and Medical Devices from the Japan Health Sciences Foundation.

Appendix

Figure with essential color discrimination. Figs. 2–4 in this article have parts that are difficult to interpret in black and white. The full color images can be found in the on-line version, at doi:10.1016/j.biomaterials.2010.09.030.

References

[1] Hanash S. Disease proteomics. Nature 2003;422(6928):226–32.
[2] Kavallaris M, Marshall GM. Proteomics and disease: opportunities and challenges. Med J Aust 2005;182(11):575–9.
[3] Oh-Ishi M, Maeda T. Disease proteomics of high-molecular-mass proteins by two-dimensional gel electrophoresis with agarose gels in the first dimension (Agarose 2-DE). J Chromatogr B Analyt Technol Biomed Life Sci 2007;849(1–2):211–22.
[4] Chaga GS. Antibody arrays for determination of relative protein abundances. Methods Mol Biol 2008;441:129–51.
[5] Kaufmann H, Bailey JE, Fussenegger M. Use of antibodies for detection of phosphorylated proteins separated by two-dimensional gel electrophoresis. Proteomics 2001;1(2):194–9.
[6] Xu ZW, Zhang T, Song CJ, Li Q, Zhuang R, Yang K, et al. Application of sandwich ELISA for detecting tag fusion proteins in high throughput. Appl Microbiol Biotechnol 2008;81(1):183–9.
[7] Au NH, Gown AM, Cheang M, Huntsman D, Yorida E, Elliott WM, et al. P63 expression in lung carcinoma: a tissue microarray study of 408 cases. Appl Immunohistochem Mol Morphol 2004;12(3):240–7.
[8] de Jong D, Xie W, Rosenwald A, Chhanabhai M, Gaulard P, Klapper W, et al. Immunohistochemical prognostic markers in diffuse large B-cell lymphoma: validation of tissue microarray as a prerequisite for broad clinical applications (a study from the Lunenburg Lymphoma Biomarker Consortium). J Clin Pathol 2009;62(2):128–38.
[9] Kozarova A, Petrinac S, Ali A, Hudson JW. Array of informatics: applications in modern research. J Proteome Res 2006;5(5):1051–9.
[10] Rimm DL, Camp RL, Charette LA, Costa J, Olsen DA, Reiss M. Tissue microarray: a new technology for amplification of tissue resources. Cancer J 2001;7(1):24–31.
[11] Tawfik El-Mansi M, Williams AR. Validation of tissue microarray technology using cervical adenocarcinoma and its precursors as a model system. Int J Gynecol Cancer 2006;16(3):1225–33.
[12] Asadi A, Pourfathollah AA, Mahdavi M, Eftekharian MM, Moazzeni SM. Preparation of antibody against horseradish peroxidase using hybridoma technology. Hum Antibodies 2008;17(3–4):73–8.
[13] Hadas E, Theilen G. Production of monoclonal antibodies. The effect of hybridoma concentration on the yield of antibody-producing clones. J Immunol Methods 1987;96(1):3–6.
[14] Makonkawkeyoon L, Pharephan S, Makonkawkeyoon S. Production of a mouse hybridoma secreting monoclonal antibody highly specific to hemoglobin Bart's (gamma4). Lab Hematol 2006;12(4):193–200.
[15] McKinney KL, Dilwith R, Belfort G. Optimizing antibody production in batch hybridoma cell culture. J Biotechnol 1995;40(1):31–48.
[16] Barbas 3rd CF, Kang AS, Lerner RA, Benkovic SJ. Assembly of combinatorial antibody libraries on phage surfaces: the gene III site. Proc Natl Acad Sci U S A 1991;88(18):7978–82.
[17] Coomber DW. Panning of antibody phage-display libraries. Standard protocols. Methods Mol Biol 2002;178:133–45.
[18] McCafferty J, Griffiths AD, Winter G, Chiswell DJ. Phage antibodies: filamentous phage displaying antibody variable domains. Nature 1990;348(6301):552–4.
[19] Okamoto T, Mukai Y, Yoshioka Y, Shibata H, Kawamura M, Yamamoto Y, et al. Optimal construction of non-immune scFv phage display libraries from mouse bone marrow and spleen established to select specific scFvs efficiently binding to antigen. Biochem Biophys Res Commun 2004;323(2):583–91.
[20] Smith GP. Filamentous fusion phage: novel expression vectors that display cloned antigens on the virion surface. Science 1985;228(4705):1315–7.
[21] Vaughan TJ, Williams AJ, Pritchard K, Osbourn JK, Pope AR, Earnshaw JC, et al. Human antibodies with sub-nanomolar affinities isolated from a large non-immunized phage display library. Nat Biotechnol 1996;14(3):309–14.